



# Water for a Healthy Country

---

## Hydrodynamic Modelling of the Coorong

---

Ian T Webster

Water for a Healthy Country

Hydrodynamic Modelling  
of the Coorong

Ian T Webster

ISBN: 978 0 643 09450 5

Water for a Healthy Country is one of six National Research Flagships established by CSIRO in 2003 as part of the National Research Flagship Initiative. Flagships are partnerships of leading Australian scientists, research institutions, commercial companies and selected international partners. Their scale, long time-frames and clear focus on delivery and adoption of research outputs are designed to maximise their impact in key areas of economic and community need. Flagships address six major national challenges; health, energy, light metals, oceans, food and water.

The Water for a Healthy Country Flagship is a research partnership between CSIRO, state and Australian governments, private and public industry and other research providers. The Flagship aims to achieve a tenfold increase in the economic, social and environmental benefits from water by 2025.

© Commonwealth of Australia 2007 All rights reserved.

This work is copyright. Apart from any use as permitted under the Copyright Act 1968, no part may be reproduced by any process without prior written permission from the Commonwealth.

Citation: Webster, I.T., 2007. Hydrodynamic modelling of the Coorong. Water for a Healthy Country National Research Flagship, CSIRO

#### DISCLAIMER

You accept all risks and responsibility for losses, damages, costs and other consequences resulting directly or indirectly from using this site and any information or material available from it.

To the maximum permitted by law, CSIRO excludes all liability to any person arising directly or indirectly from using this site and any information or material available from it.

For more information about Water for a Healthy Country Flagship visit or the National Research Flagship Initiative at [www.csiro.au](http://www.csiro.au).

Printed February 2007

## Foreword

The environmental assets of the Coorong, Lower Lakes and Murray Mouth (CLLAMM) region are currently under threat as a result of the ongoing changes in the hydrological regime of the Murray–Darling River. While a number of initiatives are underway to halt or reverse this environmental decline, such as the Murray-Darling Basin Commission’s Living Murray initiative, rehabilitation efforts are hampered by the lack of knowledge about the links between flows and ecological responses in this system.

As a component of the Water for a Healthy Country National Research Flagship, CSIRO has developed a collaborative research program with the aim of producing a decision-support framework for environmental flow management for the CLLAMM region. This involves understanding the links between the key ecosystem drivers for the region (such as water level and salinity) and key ecological processes (generation of bird habitat, fish recruitment, etc.). A second step will involve the development of tools to predict how ecological communities will respond to manipulations of the 'management levers' for environmental flows in the region. These include flow releases from upstream reservoirs, the Lower Lakes barrages, and the Upper South East Drainage scheme, and dredging of the Murray Mouth. The framework will attempt to evaluate the social, economic and environmental trade-offs for different scenarios of manipulation of management levers, as well as different climate scenarios in the Murray–Darling Basin.

The research program brings together several institutions as well as researchers from a range of backgrounds. CSIRO provides a core of expertise in the fields of hydrodynamics, biogeochemistry and socioeconomics. Knowledge about the links between ecological drivers and ecosystem responses will be developed with the CLLAMMecology research cluster, a partnership between the University of Adelaide, Flinders University and South Australian Research and Development Institute (SARDI) Aquatic Sciences supported by the Flagship Collaboration Fund.

This report is part of a series summarising the output from the Water for a Healthy Country Coorong, Lower Lakes and Murray Mouth program. Previous reports and additional information about the program can be found at [www.csiro.au/csiro/channel/ich4.html](http://www.csiro.au/csiro/channel/ich4.html).

# Contents

<b>Foreword</b> .....	<b>i</b>
<b>Abbreviations</b> .....	<b>iii</b>
<b>Acknowledgements</b> .....	<b>iv</b>
<b>1. Introduction</b> .....	<b>1</b>
<b>2. Model Description</b> .....	<b>3</b>
2.1. Site description and model domain .....	3
2.2. Hydrodynamic model .....	5
2.2.1. Equations .....	5
2.2.2. Hydrodynamic model solution .....	7
2.3. Salinity model .....	9
2.3.1. Equations .....	9
2.3.2. Salinity model solution .....	9
2.4. Model calibration .....	10
2.4.1. Calibration – step 1 .....	10
2.4.2. Calibration – step 2 .....	12
<b>3. Model–data Comparisons</b> .....	<b>14</b>
3.1. Water level .....	14
3.2. Salinity.....	17
<b>4. Coorong Dynamics</b> .....	<b>20</b>
4.1. Mouth opening dynamics.....	20
4.2. Water levels .....	22
4.2.1. Tidal water level variation.....	22
4.2.2. Wind-driven water level variation .....	24
4.2.3. Low-frequency water level variation .....	26
4.3. Water budgets in lagoons .....	28
4.4. Salinity dynamics.....	30
<b>5. Summary and Conclusions</b> .....	<b>34</b>
<b>6. References</b> .....	<b>36</b>
<b>Appendix A: Flow through a restricted channel section</b> .....	<b>38</b>
<b>Appendix B: Data sources</b> .....	<b>40</b>
<b>Appendix C: Numerical diffusion</b> .....	<b>42</b>

## Abbreviations

AHD	Australian height datum
CFMI	Computational Fluid Mechanics International
CLLAMM	Coorong, Lower Lakes, and Murray Mouth Project
Mouth	Murray River mouth
SARDI	South Australian Research and Development Institute
USE	Upper Southeast
USED	Upper South East Drainage scheme / area
MOI	mouth opening index
RMS	root mean square

## **Acknowledgements**

The author would like to acknowledge the provision of water level data for Victor Harbor by Flinders Ports Pty Ltd. (Greg Pearce) and by the National Tidal Centre (Paul Davill). Meteorological data were made available by the Bureau of Meteorology (Lynda Garlick) and data on barrage openings were provided by the Murray-Darling Basin Commission (Heather Peachey). The salinity and water level data were obtained from the Surface Water Archive (SA Department for Water, Land & Biodiversity Conservation). The author is also grateful to Kerryn McEwan for organising data acquisition from some organisations and to Sebastien Lamontagne for facilitating the project that led to this report. In his review of the report, David Walker provided many useful comments and suggestions for its improvement.

## Executive Summary

The Coorong, Lower Lakes, and Murray Mouth Project (CLLAMM) in the River Murray Theme of Water for Healthy Country was instigated to examine the relationships between manipulation of system drivers and the physical and biogeochemical responses of the Coorong. This initiative is linked directly to the CLLAMMecology Project which aims to develop an understanding of how physical manipulation of the system will impact on its ecological condition including birds and fish. Potential drivers of the system include the timing and volume of barrage flows, Upper Southeast (USE) drainage inflows, and the degree of openness of the Murray Mouth (Mouth) connecting the Coorong to the sea. Key elements of the physical condition of the system that are certain to have a direct and important effect on ecological function include water levels, salinity and the mixing conditions throughout the Coorong that determine the transport and concentrations of the nutrients that are necessary to sustain plant growth.

This report describes the development and application of a one-dimensional hydrodynamic model that will be used both to better understand and to quantify the relationship between system drivers and water levels, salinity, and mixing conditions in the North and South Lagoons of the Coorong. An anticipated future use of this model would be to support the examination of scenarios for optimisation of the benefits of system management.

This hydrodynamic model is one-dimensional along the length of the Coorong including its estuarine region and the Mouth. The model is forced by sea level changes, wind, flow through the barrages, evaporation, precipitation, exchange through the Mouth and flows from the Upper South East Drainage scheme (USED). The model simulates water levels, salinities and mixing properties along the length of the Coorong over periods of years. It does not simulate the effects of barrage flows on Mouth opening, but it does infer what the effective Mouth opening must have been to result in the measured hydrodynamic response within the Coorong.

We describe the structure of the model and discuss its calibration and validation. The calibration parameters that needed to be defined include degree of Mouth opening, effective channel width and depth of the channel connecting the North and South Lagoons, and effective evaporation rate. We also discuss major features of the physical dynamics of the Coorong that are revealed by the model application. Overall, the hydrodynamic and salinity models were well able to represent the time series of measured water levels and salinities throughout the Coorong system lending credibility to conclusions drawn from model application about the dynamics of this lagoon system.

The application of the models reinforces previous suppositions about the physical dynamics of the Coorong, and unveils some new features of their character:

1. The hydrodynamic model infers the depths of the Mouth channel from the transmission of water level variations from the sea into the Coorong. The results confirm what is already known – that barrage outflows are the agent for maintaining the Mouth in an open condition. A simple model for predicting Mouth depth as a function of Mouth flow over four years of the hydrodynamic model application is presented and well represents water level variations. It remains to be tested for other years.
2. Within the body of the North Lagoon, at weather timescales (10 days or less), water level variations are caused in similar measure by the wind which tilts the water level one way or another depending on wind direction and by sea level variations. In the South Lagoon, water level fluctuations at weather timescales are mostly caused by the wind.
3. Sea level variations having periods longer than a few days penetrate more effectively than shorter period fluctuations into the Coorong and can be important drivers of water level fluctuations and water exchange in both lagoons. The penetration of sea level variations is limited by the depth of the Mouth channel and of the channel connecting the North and South Lagoons. When sea level (and water level in the North Lagoon) drops below approximately 0 m (Australian height datum – AHD) in summer, water flow through the Parnka Point channel is not able to replenish evaporative losses in the South Lagoon resulting in a further level drop and increased salinity. Water level in both lagoons rises later in the year with the seasonal rise in sea level in autumn.

4. Salinity in the Coorong is determined by the transport of salt in water by currents, by net evaporation, and by the input of salt through the Mouth and USE drainage. Along the length of the system, evaporation tends to cause the salt concentration to increase with time. The evaporative loss of water in both lagoons requires a replacement flow along the Coorong which carries saltwater with it. At the same time, long-Coorong mixing processes transport salt towards the Mouth. Ultimately, the salinity levels in the system are determined by the balance between 'forward' transport of salt in the flow required to replace evaporation (transport towards the southeast) and the 'backward' mixing of salt by oscillatory currents induced by the wind, barrage flows and sea level changes.
5. The condition of the Mouth channel impacts on the mixing processes within the Coorong and so has a major influence on the salinity regime. When the Mouth is constricted, fluctuations in sea level penetrate less effectively into the Coorong and the exchange flows associated with these level fluctuations are reduced. As a consequence, mixing of salt back towards the Mouth is less effective and salinity tends to increase in both lagoons.
6. The barrage flows influence the salinity dynamics in the Coorong in at least three important ways. Periods of elevated barrage flows deepen the Mouth channel which in turns allows more active mixing along the length of the Coorong. By freshening the water at the northern end of the North Lagoon (compared to sea water), the water that flows along the Coorong to replace evaporative losses has a lower salinity. When the barrages flow, the water level in the whole system tends to increase and water is pushed along the Coorong. Generally, variations in discharge cause the water level in the Coorong to rise and fall causing back and forth water exchange along the system which enhances longitudinal mixing.

# 1. Introduction

The Coorong, Lake Alexandrina, Lake Albert, and Murray Mouth form a terminal lakes system at the mouth of the River Murray in South Australia (Figure 1). A line of barrages inside the mouth separates the lower lakes (Alexandrina and Albert) from the saline waters of the Coorong that exchange with the sea through the Murray Mouth (Mouth). The barrages prevent seawater from entering the lakes and lower Murray, and maintain higher water levels in the naturally shallow Lakes. During times of high discharge in the Murray, significant volumes of fresh water pass the barrages and these flows have been deemed essential for maintaining the Murray Mouth in an open condition. Over the past decades, flows in the River Murray have been reduced to a fraction of previous volumes mainly due to irrigation abstraction and it would appear that the likelihood of Mouth closure has increased over this time as a consequence.

The Coorong is a lagoon system several kilometres wide that follows the coast for more than 100 km from the Mouth. It is divided into the North and South Lagoons by significant reductions in channel width and depth near Parnka Point (Figure 1). The Coorong and the Lower Lakes are of national and international conservation status especially for birds, the Coorong being ranked within the top six waterbird sites in Australia. These water bodies are Ramsar listed and are listed as one of six Significant Ecological Assets identified in the Living Murray Initiative (<http://www.thelivingmurray.mdbc.gov.au/>).



**Figure 1. The Coorong, Lower Lakes and Murray Mouth.**

Reduced river flows and the associated increased likelihood of Mouth closure are regarded as a threat to the ecological function of the Coorong through the propensity for higher salinities in the system, alterations to the water level regime and blockage of fish migration pathways. There are a number of ways the physical environment of the Coorong can be altered through human manipulation. These drivers include dredging the Mouth when it is threatened by closure and altering the timing and magnitude of flows past the barrages and releases from the Upper South East Drainage scheme (USED) into the southern end of the South Lagoon at Salt Creek.

The Coorong, Lower Lakes, and Murray Mouth Project (CLLAMM) in the River Murray Theme of Water for Healthy Country Flagship was instigated to examine the relationships between manipulation of system drivers, and the physical and biogeochemical responses of the

Coorong. The aims, rationale, and context of the CLLAMM project are outlined by Lamontagne et al. (2004). As part of this project, summary reports on system hydrodynamics (Webster 2005) and on system biogeochemistry (Ford 2007) have been prepared. This work is being extended through the development of hydrodynamic and biogeochemical models that will be used for system diagnoses as well as prediction of the likely effects of future management action on water levels, salinity, nutrient concentrations and primary production. The ecological function of the Coorong is being investigated through the CLLAMMecology initiative, a consortium of researchers from the University of Adelaide, Flinders University, South Australian Research and Development Institute (SARDI), and SA Water. The ecological impact of driver manipulation will largely be a consequence of alterations that occur to the physical and biogeochemical alterations to the system and will be at least partly understood and predicted in this context.

This report describes the development and application of a one-dimensional hydrodynamic model of the Coorong which is the next stage of the CLLAMM project. The model aims to develop simulations of water level regime and salinity along the length of the Coorong as these respond to manipulation of barrage flows, USED flows and Mouth opening. Water level is a key environmental attribute that determines the availability of physical habitat for birds and for other aquatic life. Similarly, all aquatic organisms have tolerance limits to salinity levels and their degree of variation, so the salinity regime within the Coorong is a major determinant of where and how well such organisms can live and prosper. A third purpose of the hydrodynamic modelling is the diagnosis and quantification of water exchange along the Coorong which will be a key element in the successful application of the biogeochemical model to be next developed. The biogeochemical model will predict nutrient concentrations as well as the growth rate and form of primary producers along the Coorong. As food for higher trophic levels, phytoplankton and aquatic plants are key determinants of ecological dynamics.

The hydrodynamic model described here is one-dimensional along the length of the Coorong including its estuarine region and the Murray Mouth. Its fundamental dynamics are similar to those employed by Computational Fluid Mechanics International (CFMI) in its modelling of the hydrodynamics and salinity levels in the Coorong (CFMI 1992, CFMI 1998, CFMI 2000), but this modelling did not extend to the Murray Mouth. The model we implement here is forced by sea level changes, wind, flow through the barrages, evaporation, precipitation, exchange through the Mouth and flows from the USED. The model simulates water levels, salinities and mixing properties along the length of the Coorong over periods of years. It does not simulate the effects of barrage flows on Mouth opening, but it does infer what the effective Mouth opening must have been to result in the measured hydrodynamic response within the Coorong. A three-dimensional morphological model that couples hydrodynamics and sediment dynamics has been developed and applied by WBM Oceanics to simulate the response of the Mouth opening to flow and wave conditions around the Mouth (WBM Oceanics 2003).

In the following report, the structure of the model is described followed by discussion of its calibration, validation and application.

## 2. Model Description

### 2.1. Site description and model domain

The Coorong naturally splits into North and South Lagoons at Parnka Point (Figure 1). There are several channel sections on either side of Parnka Point that are very narrow (approximately 100 m) and shallow, and that represent the main restriction for water exchange between the two lagoons (Figure 2). The length of the North Lagoon to the Mouth is approximately 60 km versus a length of approximately 40 km for the South Lagoon. At zero water elevation (Australian height datum – AHD), the average widths of the North and South Lagoons are 1.5 km and 2.5 km, respectively, whereas the average depths are 1.2 m and 1.4 m, respectively (CFMI 1992). The respective volumes of the North and South Lagoons are  $86 \times 10^6 \text{ m}^3$  and  $140 \times 10^6 \text{ m}^3$ .

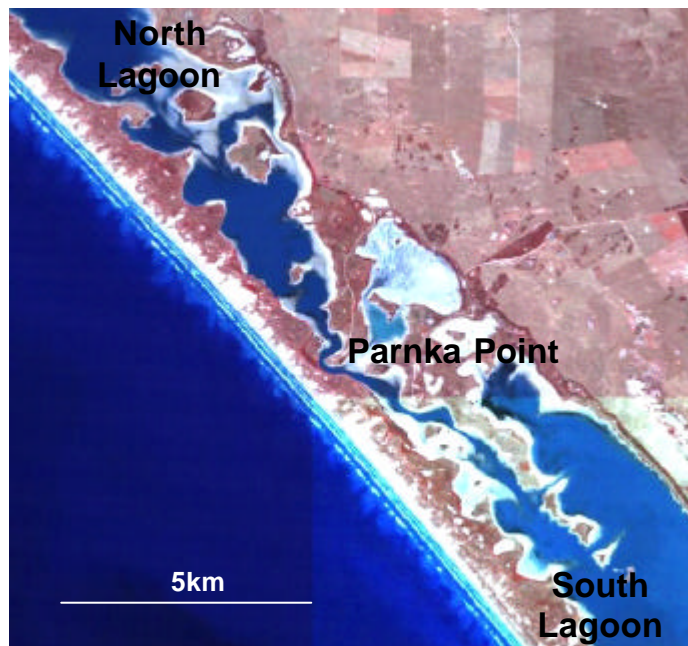


**Figure 2. ASTER image of Coorong channels near Parnka Point – 4 November 2003.**

The sole connection of the Coorong to the sea occurs through the Murray Mouth near the northwest end of the North Lagoon (Figure 1 and Figure 3). The Mouth has always been relatively narrow, but it has been and continues to be extremely dynamic. The width of the Mouth has varied from being several hundred metres during flood flows (Walker 2002), but it was closed completely in 1981 and almost closed in 2003. Given micro-tidal conditions and domination of wave energy along the coast, a flood-tide delta (a delta landward of the Mouth) is to be expected and does occur in this system (Harvey 1996).

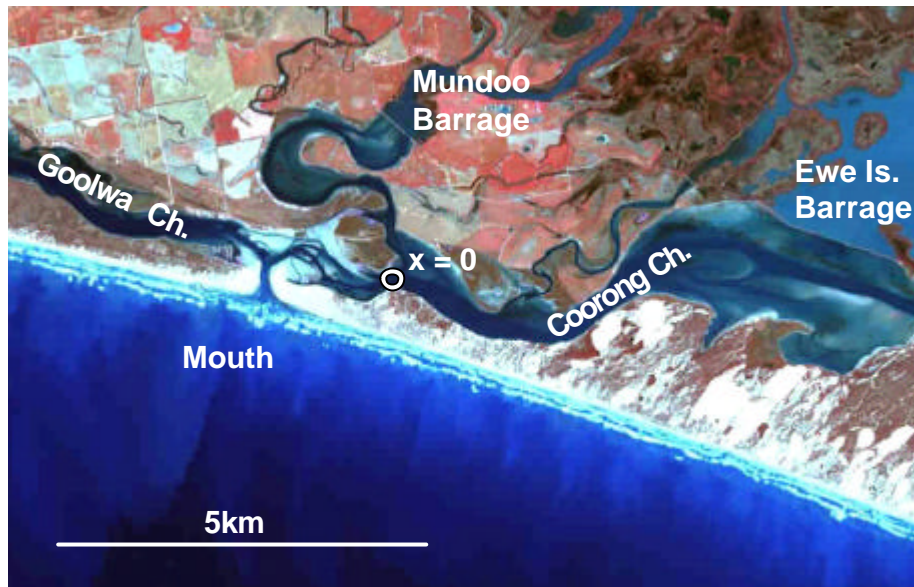


**Figure 3. ASTER image of Coorong near the Mouth – 4 November 2003.**

The main body of the Coorong lies to the southeast of the Mouth and is connected to the Mouth via the Coorong Channel. Goolwa Channel, a smaller section of the Coorong, runs approximately 8 km towards the northwest from the Mouth where it ends at Goolwa Barrage. The most severe constrictions in Goolwa and Coorong Channels occur where these channels cross the delta opposite the Mouth. It is in these channel sections that dredging has been undertaken since 2003 to maintain an open connection between the Coorong and Encounter Bay.



**Figure 4. Photograph of the Mouth looking towards the northwest (26 November 2003). The channel being dredged between Coorong Channel and the Mouth curves around the right hand side of the sand bank in the lower centre part of the photograph.**

The flow through the barrages separating the Coorong from Lake Alexandrina can be controlled individually by raising or lowering gates, but for most of the time these flows are zero. Releases of water depend very much on flow conditions in the River Murray and in recent years these flows have been reduced due to drought conditions. During 2002 and 2003, there has been virtually no fresh water released past the barrages. Most releases occur through the three main barrages namely Goolwa, Ewe Island and Tauwitchere Barrages. Near the southern end of the South Lagoon, additional discharge to the Coorong has occurred through Salt Creek in recent years. This water is surface drainage water from the Upper Southeast Drainage scheme (USED) that has been collected via a network of channels into Morella Basin where it is stored

before release. These releases have occurred in late spring – early summer. The system connectedness is schematicised in Figure 5.

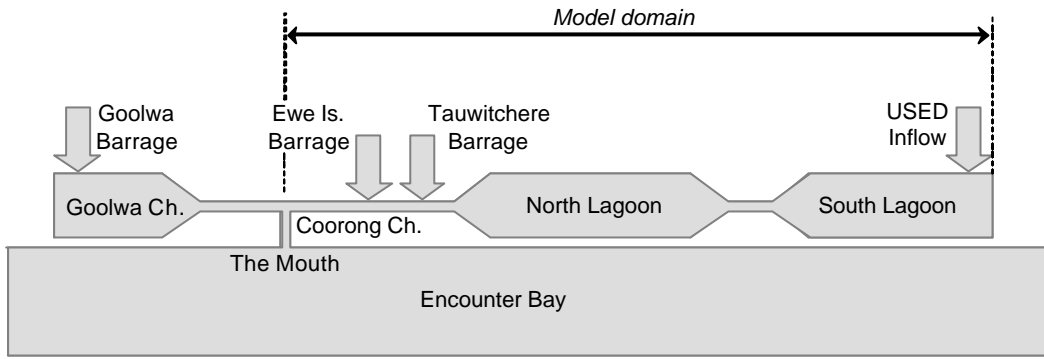


**Figure 5. Coorong connectedness including major inflows.**

The zone considered for modelling in this report extends from the Mouth through both North and South Lagoons. The CFMI (1992) modelling domain covered most of this area, but its northern extent reached Pelican Point at the eastern end of Tauwichee Barrage (Figure 1) and did not include modelling of the Mouth region and much of the estuary. By including the Mouth, we are able to simulate the behaviour of water levels and salinities along the North and South Lagoons as these respond to changes in the exchanges through the Mouth and variations in sea level. The WBM Oceanics model's domain (WBM Oceanics 2003) includes Goolwa Channel and simulates how barrage flows impact on Mouth opening, so in these respects, it is more extensive than the modelling that we undertake here. Conversely, the one-dimensional model is many times faster which allows it to be run for many more scenarios over much longer time periods than the three-dimensional hydrodynamic-geomorphological model.

## 2.2. Hydrodynamic model

### 2.2.1. Equations

The Saint-Venant equations for mass and momentum conservation can be written as (Cunge et al. 1980, Crossley 1999):

$$\frac{\partial A}{\partial t} + \frac{\partial Q}{\partial x} = \frac{\partial Q_{in}}{\partial x} \quad (1)$$

and:

$$\frac{\partial Q}{\partial t} + \frac{\partial}{\partial x} \left( \frac{Q^2}{A} \right) + gA \frac{\partial \eta}{\partial x} + gAS_f = \frac{W\tau_x}{\rho_w} \quad (2)$$

The variables are defined in Table 1. Over most of the model domain, the non-linear terms in Equation 2 can be neglected so that the equation is simplified to:

$$\frac{\partial Q}{\partial t} + gA \frac{\partial \eta}{\partial x} + gAS_f = \frac{W\tau_x}{\rho_w} \quad (3)$$

Variable	Description
$A(x, t)$	cross-sectional area of the Coorong
$D$	dispersion coefficient used in salinity model
$H(x, t)$	water depth = $H_0(x) + \eta(x, t)$ ; $H_0(x)$ is water depth at $\eta = 0$
$P$	pan evaporation correction factor
$Q(x, t)$	flow volume along Coorong
$Q_{in}(x, t)$	accumulated inflow to Coorong (from $x = 0$ )
$R(x, t)$	hydraulic radius taken to be water depth
$S(x, t)$	salinity in water column
$S_{in}(x, t)$	salinity of inflow to Coorong
$t$	time
$x$	distance measured along the Coorong from the Mouth (see Figure 3)
$W(x)$	local width of Coorong
$W_{PP}, W_M$	widths of Parnka Point and Mouth channels
$Z_{PP}, Z_M(t)$	bed heights of Mouth and Parnka Point channels
$\eta(x, t)$	elevation of the water surface (AHD)
$\tau_x$	component of wind stress along axis of Coorong

**Table 1. Principal variables used in report.**

$Q_{in}$  is total inflow accumulated along the Coorong from  $x = 0$  and is comprised of flows through the barrages, the USED inflow, and a contribution from precipitation (positive) and one from evaporation (negative). The friction slope is represented using Manning's equation and is expressed as:

$$S_f = \frac{n^2 Q |Q|}{A^2 R^{4/3}} \quad (4)$$

where  $n$  is Manning's friction coefficient and  $R$  is the hydraulic radius. The appropriate value of  $n$  depends on bottom roughness and also, to a significant extent, on flow speed. For flows over sand for example, the bottom shape may change from flat to dunes as the flow speed is changed. This change in bedform affects its frictional characteristics (Arcement and Schneider 1984). WBM Oceanics (2003) investigated the effect of  $n$  on model agreement with measured water levels and found that values of  $n$  between 0.02 and 0.03 were appropriate for the Coorong. We choose a middle value of  $n = 0.025$  (SI units). The hydraulic radius is the ratio of the cross-sectional area of a channel to its wetted perimeter. For a channel whose width is much larger than its depth,  $R$  is very close to the water depth averaged across the channel width so we set  $R = \bar{H}$ .

In the following report, for ease of nomenclature, we will refer to the constricted channel section connecting the western end of the Coorong Channel and the sea as the Mouth channel and the constricted channel sections near Parnka Point as the Parnka Point channel. For the hydrodynamics, Equations 1 and 3 were the equations solved over most of the model domain except for the Mouth and Parnka Point channels.

Note that the references to Mouth opening by Walker (2002) and by Shuttleworth et al. (2005) really pertain to the channel sections connecting the Goolwa Channel to the sea.

A site visit to the Mouth area during 2003 during an outflowing tide suggested that at times the flow through this channel section was subject to 'upstream' hydraulic control. In effect, the channel was shallow enough at this time and the flow rate high enough that there appeared to be a substantial water level drop moving from the upstream end of the channel to its downstream end. The flow appeared to tumble downwards over its bed and had the appearance of rapids.

Under low flows, the discharge through a channel is related to both the upstream and downstream water elevations, but under conditions of high discharge and low downstream water level, the flow volume may be determined by the upstream water level only; that is, the flow is subject to upstream hydraulic control. An extreme example of this type of flow is the waterfall. In Appendix A, we outline the method used to determine the flows through the constricted Mouth and Parnka Point channels when they are subject to upstream hydraulic control.

For the fully calibrated hydrodynamic model, the flow through the Mouth was restricted to a maximum by upstream hydraulic control for 4% of the time, but the rate of water exchange between the North and South Lagoons was limited to a maximum by upstream hydraulic control for 7% of the time. Upstream hydraulic control in these channels is most important for restricting flows when the channels are shallow and its occurrence is an important feature of the hydrodynamics of the Coorong system.

### 2.2.2. Hydrodynamic model solution

The grid established for the hydrodynamic model uses a 1-km grid cell with  $x = 0$  close to the Mouth and  $x$  increasing towards the southern end of the Coorong. The model grid extends to 6 km beyond Salt Creek making a domain length of 102 km (see Figure 6 for schematic diagram).

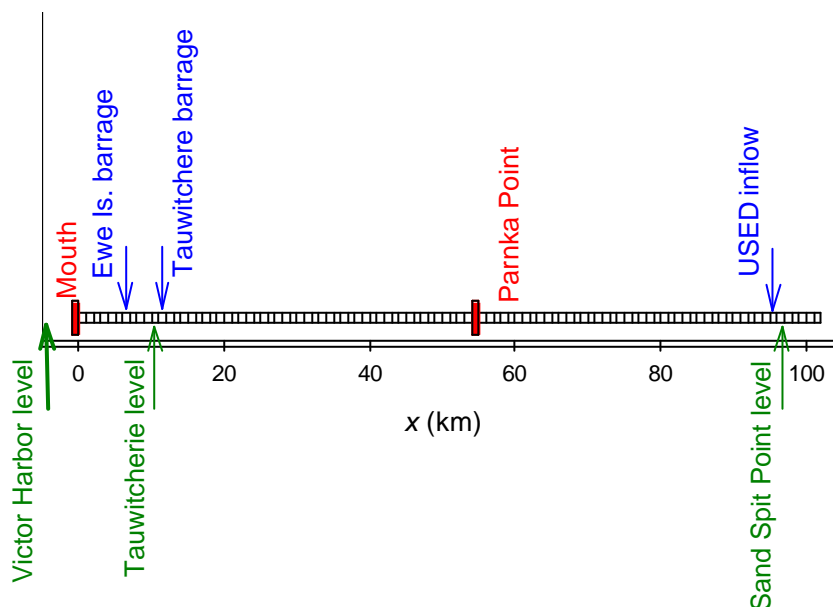


**Figure 6. Schematic of grid scheme used in hydrodynamic model. The cells marked in red are the two major constrictions that are considered differently from the rest of the grid.**

The model Equations 1 and 3 were represented in finite-difference form on this grid. The time-derivative terms were represented in forward-difference form and the spatial gradients as central differences (Roache 1982). From initial water levels specified for the North and South Lagoons, the model solution comprising simulated water level ( $\eta$ ) and flow ( $Q$ ) was stepped

forward in time. The flows through the two constrictions were calculated at each time step from the water elevations in the cells on either side.

In the South Lagoon, bathymetric data were available at cross-sections measured at an approximately two-kilometre spacing along the lagoon. For some transects, the lateral distance between depth measurements was hundreds of metres. In the North Lagoon, more recently collected bathymetric data were used with lateral and longitudinal spacing of 50 m or less. For both lagoons, the bathymetric data were interpolated onto the model grid and averaged laterally to provide average water depth as a function of water level. Generally, the average water depth does not change at the same rate as water level; the relationship between the two depending on the hypsometric curve. Initially, we used lagoon widths that depended on water level which results in a non 1:1 relationship between changes in water depth and water elevation. Later, this scheme was changed to one in which the lagoon widths were held constant. In effect, the lagoon was considered to have vertical walls. This assumption is not so accurate, but it led to more robust model solutions while maintaining satisfactory results. The lagoon width at each grid cell was taken to be the width derived from the measurements at a water level of  $\eta = 0.2\text{m}$ . This is the average measured water level of the Coorong. The average water depth at each grid cross section was calculated at this water level. Thus, the average depth at another level (in metres) is calculated as:

$$H_{\eta} = H_{0.2} - 0.2 + \eta \quad (5)$$

The measured water level at Sand Spit Point in the South Lagoon reduced to less than -0.4 m in 2003. Such low water levels caused problems for model stability during times of high wind stress due to tilting of the water surface. Consequently, we chose to limit the minimum depth at  $\eta = 0$  (AHD) to 0.8 m. The width and depths used for the final model applications are shown in Figure 7.

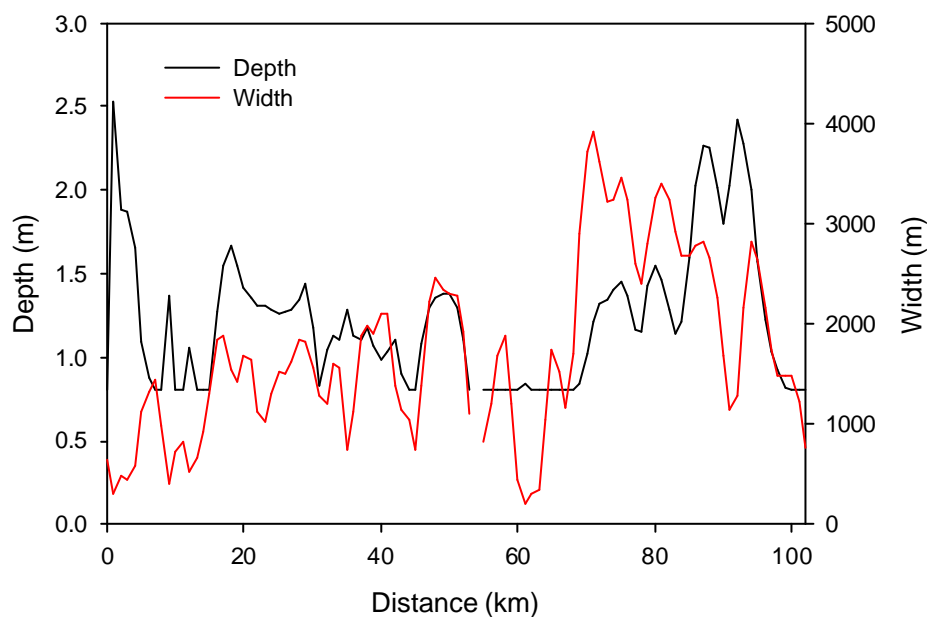


**Figure 7. Widths and depths as used in model application. Depths are referenced to AHD ( $h = 0$ ).**

Input data required to drive the model and water levels required to validate and calibrate it were available from a number of sources. The model was forced by the time varying water level in Encounter Bay, by the inflows through the barrages and from the USED, by evaporation and precipitation, and by wind stress. Water levels measured at Tauwichee and at Sand Spit Point were used to calibrate the model. The time series of forcing functions were obtained from a number of sources and in some cases required some manipulation to reduce them to the required form. Details of data sources and manipulation are outlined in Appendix B. The calibration of the model and its implementation require continuous records of water levels measured at Victor Harbor and inside the Coorong at Tauwichee Barrage. Consequently, the

time period for our application is restricted by data availability to the period between mid-August 1998 to the end of February 2004 with some relatively small gaps in between.

## 2.3. Salinity model

### 2.3.1. Equations

We consider the equation for the salt balance in the Coorong to be:

$$\frac{\partial AS}{\partial t} + \frac{\partial QS}{\partial x} = \frac{\partial}{\partial x} \left( AD \frac{\partial S}{\partial x} \right) + \frac{\partial Q_{in} S_{in}}{\partial x}, \quad (6)$$

where  $S(x, t)$  is salinity,  $D$  is a turbulent dispersion coefficient for salt,  $Q_{in}$  is accumulated inflow and  $S_{in}$  is the salinity of this inflow (Officer and Lynch 1981).

### 2.3.2. Salinity model solution

A salinity measurement program comprised of intermittent surveys along both lagoons has been undertaken since 1997 by government agencies in South Australia (Appendix B). For the salinity solution, the grid that was used comprised 14 cells along the length of the Coorong with the boundaries of most cells set to lie approximately halfway in between the stations at which salinity measurements were obtained. Thus, these cells each contain one salinity sampling station. In addition, two grid cells were specified for the end of the Coorong near the Mouth without salinity sampling stations (Figure 8).

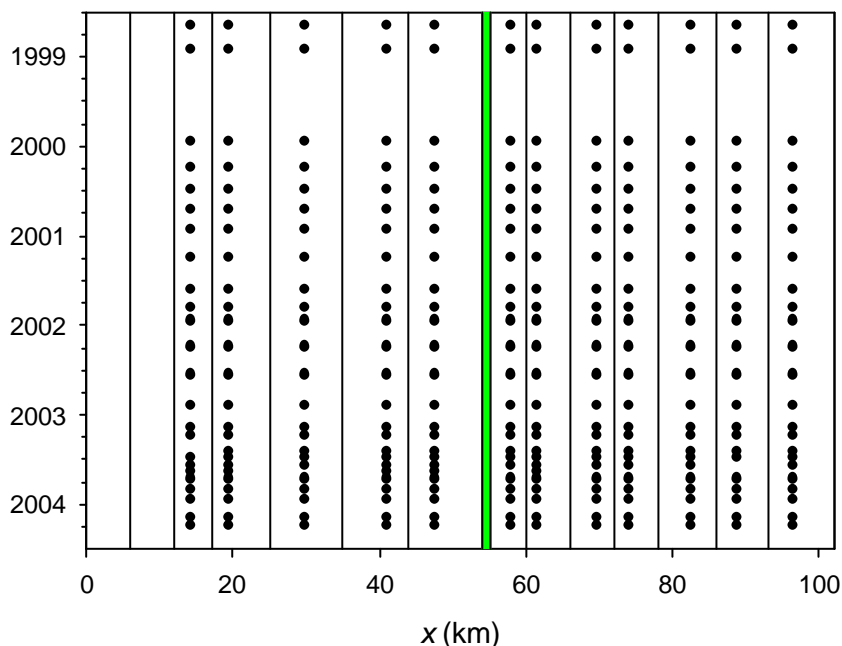


**Figure 8. Schematic showing locations of cell boundaries used in the salinity model. Also shown are the locations and times of the salinity measurements used in the calibration of the salinity model. The green band shows the location of the Parnka Point channel.**

The first term in Equation 6 was discretised in forward-time form, the second term as an upwind difference, and the third and fourth terms as central differences. The salinity equations were embedded with the hydrodynamic model equations and solved alternately. The hydrodynamic model provided the values of  $Q$  at the boundaries of the salinity cells and the water levels in their interiors. The boundary conditions for the salinity model at the start of the simulation were derived from the measurements along the length of the Coorong close to this time. The salinity

assumed for the ocean off the Mouth is a constant 35.66, a value estimated from the World Ocean Atlas 1998 (NODC 1998). The boundary condition at the southern end of the Coorong is that the flux of salt be zero at  $x = 102\text{km}$ . The salinity of the inflows associated with precipitation and the salinity of the barrage inflows are all assumed to be zero. The salinity of the USED inflow was set to 10.6 calculated as the flow weighted average of the available measurements. Salinity in the inflow was measured to vary between 4 and 13, but the volume of the USED flow was small enough that an error of 50% in the assumed salinity would have negligible impact on the modelled salinity in the Coorong.

## 2.4. Model calibration

The calibration of the hydrodynamic and salinity models for the Coorong was undertaken in two stages:

1. calibration for parameters that describe the time varying depth and width of the constricted Mouth channel connecting the Coorong to the sea
2. calibration for the depth of the Parnka Point channel, for the evaporation rate and for the longitudinal dispersion coefficient that characterises mixing along the lagoons.

Since the choice of parameters determined from each calibration affects the model simulation over the whole of the Coorong, the calibration cycle was applied twice.

### 2.4.1. Calibration – step 1

The method for determining the time series of Mouth width and bottom height was similar in principle to that employed by Walker (2002) for estimating the mouth opening index (*MOI*). We assume the Mouth channel to be approximately 1.5 km long based on satellite images. The channel will be assumed to have width  $W_M(t)$ . The height of the bottom of this channel with respect to AHD is defined as  $Z_M(t)$  so that  $-Z_M$  is the water depth at a water level of 0 m AHD ( $\eta = 0$ ). Note that by fixing the height of the bottom of the channel, the water depth within the channel rises and falls with sea level. Effectively, the first calibration stage involved determining the time series of  $W_M$  and  $Z_M$  by adjusting these two parameters to obtain an optimal fit between measured and modelled water levels at Tauwitschere.

For a particular  $W_M$  and  $Z_M$ , a model solution was calculated. Suppose the modelled and measured (data) time series of water levels at Tauwitschere are  $\{\eta_{Tm}\}$  and  $\{\eta_{Td}\}$ , respectively which have elements such that if  $\eta_{Td}^i$  is measured level at time  $t_i$ , then  $\eta_{Tm}^i$  is simulated water level at the same time. The difference time series is formed from the elements:

$$\Delta_T^i = \eta_{Td}^i - \eta_{Tm}^i \quad (7)$$

We can form low-pass and high-pass filtered time series from  $\{\Delta_T\}$  defined as  $\{\tilde{\Delta}_T\}$  and  $\{\tilde{\tilde{\Delta}}_T\}$  respectively. The cut-off period of the filter used is 48 hours. For each pair of channel parameters  $W_M$  and  $Z_M$ , we calculate the RMS (root mean square) error of the low and high-pass filtered model solutions for successive seven-day periods as:

$$\tilde{\delta}_T = \frac{1}{N} \sum_{i=l}^{l+N} (\tilde{\Delta}_T^i)^2 \quad \text{and} \quad \tilde{\tilde{\delta}}_T = \frac{1}{N} \sum_{i=l}^{l+N} (\tilde{\tilde{\Delta}}_T^i)^2 \quad (8)$$

where  $l$  is the time index of the start of the seven-day period and  $N$  is the number of measurements within this period.

The optimum  $W_M$  and  $Z_M$  for each week is determined as those values that minimise  $\tilde{\delta}_T$  and  $\tilde{\delta}_T$ . Initially, we allowed  $W_M$  and  $Z_M$  to vary independently of one another. This analysis resulted in  $Z_M$  varying quite markedly from week to week with corresponding inverse variation in  $W_M$ . That is, a sudden increase in the depth of the channel would correspond to a sudden decrease in width and vice versa. This variation occurred in such a way that the cross-sectional area of the Mouth channel tended to be preserved approximately from week to week. Such short-term changes in channel bottom height and width did not seem physically reasonable so it was next assumed that the width of the channel remained constant over the modelling period. For each week and for specified  $W_M$ , the optimum  $Z_M$  was calculated by minimising  $\tilde{\delta}_T$  and  $\tilde{\delta}_T$ . In turn, the optimum  $W_M$  was chosen as that value that minimised the sum over the whole period of the optimised  $\tilde{\delta}_T$  and  $\tilde{\delta}_T$ . For the Mouth channel, the optimum width was determined to be  $W_M = 100\text{m}$  to the nearest 10m.

Another prescription for channel width was tested which assumed the width to be a linear function of channel depth, but this approach produced only an insignificant improvement in the model fit and was discarded in the interests of maintaining simplicity in channel definition.

Figure 9 shows the time series of  $Z_M$  calculated using both the low and high-frequency analyses. In effect, the high-frequency analysis results in channel depths that derive from fitting the diurnal and semi-diurnal tidal signals at Tauwitchere whereas the low-frequency analysis fits the response due to the passage of weather systems of duration longer than a few days. The gaps in the time series are due to sections where the level data from Tauwitchere are missing. Both analyses show  $Z_M$  to range from values of over 0 m representing a severe constriction of the Mouth channel to down to -3 m representing a much more open condition. Mostly, the two analyses follow one another fairly well. The high-frequency heights show smoother variations when  $Z_M < -0.5\text{m}$ , but for larger values of  $Z_M$ , the low-frequency analysis shows more smoothly varying results. As we will show, the transmission of tides through a shallow channel is less effective than the level fluctuations of lower frequency. Consequently, when the channel becomes shallow, the optimisation technique for the tidal analysis becomes relatively more subject to 'noise' such as due to wind-driven level fluctuations. Thus, the  $Z_M$  used in further model applications will be those obtained from the high-frequency analysis for  $Z_M < -0.5\text{m}$  and from the low-frequency analysis for  $Z_M \geq -0.5\text{m}$ .

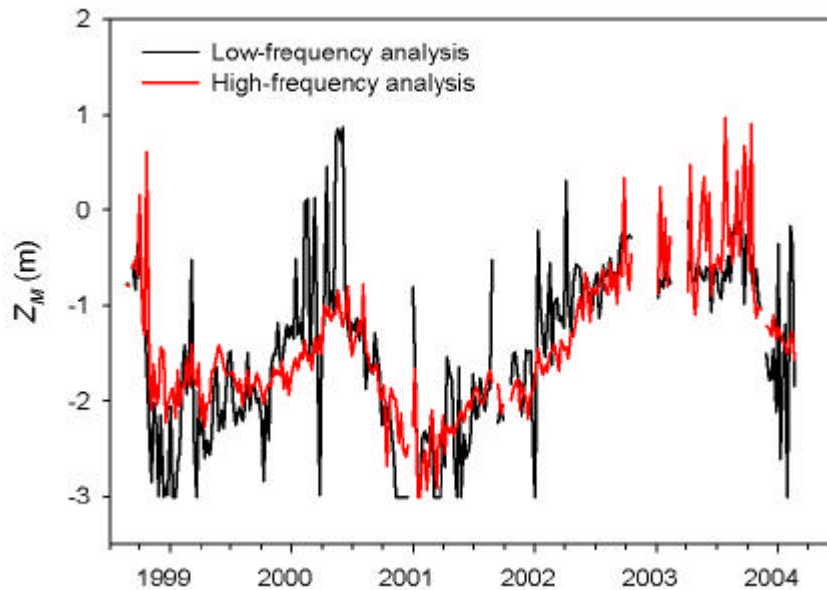


**Figure 9. Time series of heights of the Mouth channel bed (AHD) for a constant channel width of 100 m.**

### **2.4.2. Calibration – step 2**

The Parnka Point channel connecting the North and South Lagoons is shallow and narrow and has a bathymetry that is not well resolved by the available measurements. It is not clear whether the most severe constriction in this channel occurs a few kilometres to the northwest of Parnka Point or in the channel sections adjacent to Parnka Point (see Figure 2).

However, the Parnka Point channel as implemented in the model has a length of 1 km and a width of 100 m. These dimensions were approximately consistent with what might be estimated from satellite images. The height of the channel bottom ( $Z_{PP}$ ) will also be assumed to be constant, but its value is determined by a fitting procedure. During the summer months, the water level in the Coorong drops as sea level drops and barrage flows diminish (Webster 2005). Once the water level drops to  $\eta \sim 0$ , the channel connecting the lagoons becomes shallow enough that it cannot support a flow sufficient to replenish the evaporation loss from the South Lagoon. Consequently, the water level in the South Lagoon continues to drop below the level in the North Lagoon. Under these conditions, water level in the South Lagoon is determined by both the evaporation rate and by the height of the Parnka Point channel bottom. We estimate the daily evaporation rate from measurements of pan evaporation at Mundoo. Generally, pan evaporation overestimates the evaporation rate that would occur from a large open water surface such as a lake. The pan evaporation factor, which is used to adjust pan evaporation rate to that from an open surface, is usually taken to have a value of about 0.7 (Stanhill 1976, Linacre 2005). Actual pan factors may differ from this value due to effects arising from meteorological conditions and the size and geometry of the waterbody (Condie and Webster 1997). Rather than prescribing a pan evaporation factor ( $P$ ), we treat it as a parameter to be fitted.

Salinity in the Coorong is determined by the net inputs/outputs of water through barrage releases, evaporation, precipitation, Mouth flows and USED inflows. Its distribution along the Coorong is also determined by how water is mixed along the length of each lagoon and between the two lagoons. There is inherent mixing in the numerical scheme chosen for the model through numerical dispersion (Roache 1982), but additional dispersion is required to properly simulate both the temporal and spatial variations in salinity. We choose the dispersion coefficient ( $D$ ) in Equation 6 as a fitted parameter. For calibration stage 2, we calculate the RMS

deviation between measured and modelled salinity through both lagoons as  $\delta_s$ . The measurements are those obtained from the surveys along the lagoons whose times and locations are schematicised in Figure 8.

Water level was measured at hourly intervals at Sand Spit Point near the southern end of the South Lagoon for most of the modelled period. If we let  $\delta_{SP}$  be the RMS deviation between measured and modelled levels at this site and let  $\sigma_s$  and  $\sigma_{SP}$  be the standard deviations of the salinity measurements and of the measured water levels at Sand Spit Point, then we can define the stage-two error parameter for a particular model simulation as:

$$\delta_2 = \sqrt{\frac{\delta_s^2}{2\sigma_s^2} + \frac{\delta_{SP}^2}{2\sigma_{SP}^2}}. \quad (9)$$

Stage 2 calibration involved finding the optimal set of values for  $Z_{pp}$ ,  $P$  and  $D$  by running the model many times with various combinations of values for these parameters. The optimal parameter values were  $Z_{pp} = -0.30\text{m}$ ,  $P = 0.78$ , and  $D = 37\text{m}^2\text{s}^{-1}$ . A  $Z_{pp}$  of  $-0.30\text{m}$  is consistent with the observation that the channel connecting the two Coorong lagoons dries on occasion. A value for the pan evaporation factor of 0.78 is not atypical of values that have been reported for lakes. Added to the contribution from numerical diffusion of  $73\text{m}^2\text{s}^{-1}$  (see Appendix C), the horizontal diffusivity within the Coorong is  $\sim 110\text{m}^2\text{s}^{-1}$ . Estimated turbulent diffusivities for other estuaries display a range of values presumably reflecting differing channel dimensions and flows. Most of these calculations are based on salinity distributions. Examples of diffusivity estimations include those by Bowden (1965) who calculated a diffusivity of  $170\text{m}^2\text{s}^{-1}$  for the Mersey Estuary. Elliott (1976) estimated diffusivities at a number of stations for the Upper Potomac Estuary to fall in the range  $93\text{--}280\text{m}^2\text{s}^{-1}$  and Webster et al. (1994) estimated an average diffusivity of  $122\text{m}^2\text{s}^{-1}$  for the Bega estuary. Our estimated average horizontal diffusivity falls within the overall range of the diffusivities reported for estuaries.

### 3. Model–data Comparisons

This section illustrates the performance of the model through example comparisons of simulation results with measurements.

#### 3.1. Water level

Figure 10 compares the modelled and measured low-pass filtered water levels at Tauwitschere and measured Victor Harbor levels for a one-year period that typifies the whole record. The cut-off period for the filter is 2.5 days. The model reproduces the measurements well overall. The agreement is best for the first five months. This is a time when the Mouth channel is relatively deep (see Figure 9) so that one might expect a 'better connection' between the Coorong and Encounter Bay. Later in the year, the measured water levels in the Coorong are significantly higher compared to those in Encounter Bay. This is a feature that is well captured in the model simulations and is due to elevated discharges through the barrages that cause the water level to 'back-up' in the Coorong.

On an open coast such as that near the Mouth of the Coorong, waves running up the beach would be expected to cause an increase in average water level greater than that recorded at Victor Harbor – by perhaps tens of centimetres (Nielsen 1988). The swell is dominated by waves from the south west and peak during April to September (Short and Hesp 1980) so wave set-up makes a contribution to the rise in water levels in the Coorong during this time which is not accounted for in the model. How such wave set-up would interact with a channel through the beach such as at the Mouth is not known.

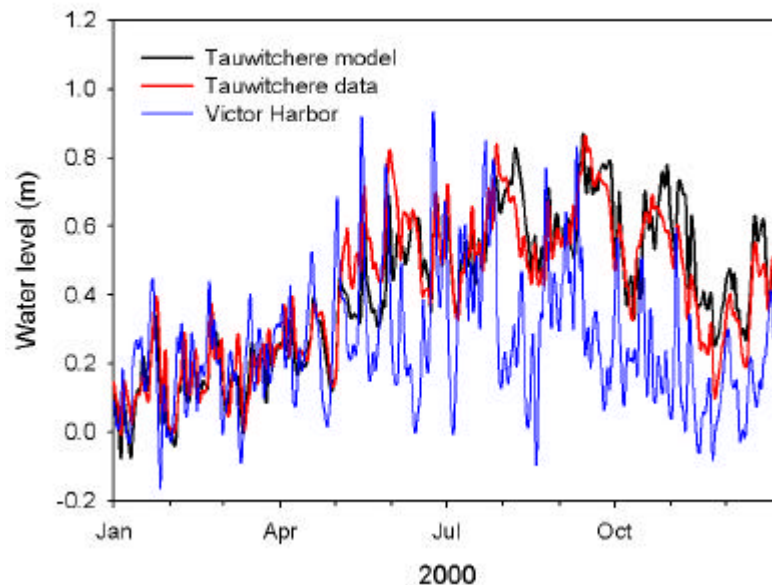


**Figure 10. Low-pass filtered modelled and measured water levels at Tauwitschere. Also shown are filtered measured water levels for Victor Harbor.**

The comparison between measured and modelled low-pass filtered water levels near the southern end of the South Lagoon at Sand Spit Point is very good (see Figure 11). The water levels in the North Lagoon do not depress much below  $\eta = 0$  (see Figure 10), but evaporation typically causes water levels in the South Lagoon to reach  $\eta \sim -0.2\text{m}$  in late summer (Webster 2005). The ability of the model to successfully simulate the depression in water level at this time depends critically on the selection of the bed height of the Parnka Point channel ( $Z_{PP}$ ).

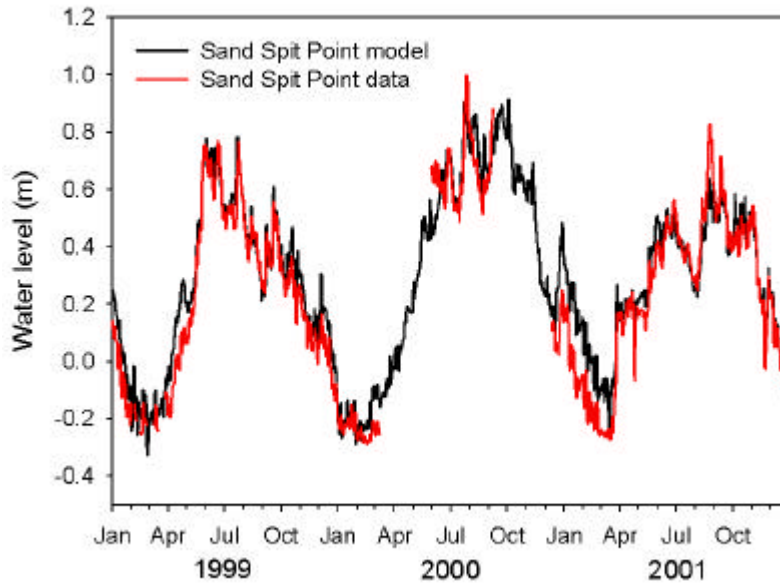


**Figure 11. Low-pass filtered modelled and measured water levels at Sand Spit Point.**

The high-pass model-measurement comparisons are presented in Figure 12 for Tauwitchere. The cut-off period for the filter is 2.5 days. The model captures the penetration of the tidal signal into the Coorong reasonably well. At this time, the Mouth is fairly open. However, at Sand Spit Point it is evident that the model attenuates the measured levels severely (Figure 13). The attenuation of the variance at high frequencies is clearly seen in the spectrum of modelled water levels for Sand Spit Point (Figure 14). For periods shorter than about two days, the modelled spectrum falls below the spectrum of measured levels. The spectra of modelled and water levels for Tauwitchere match at the diurnal and semi-diurnal (tidal periods), but a significant reduction in the modelled spectrum below the measured spectrum occurs at neighbouring frequencies. The explanation is the misrepresentation of the true wind stress in the model at higher frequencies. Wind stress was derived from only two measurements per day at 9 am and 3 pm, so this time series is not capable of adequately representing variance at periods of less than two days. The loss in variance in wind stress at high frequencies is clearly seen in the drop in its spectrum (Figure 14). Model performance at higher frequencies would be greatly improved if meteorological data of higher temporal resolution were available.

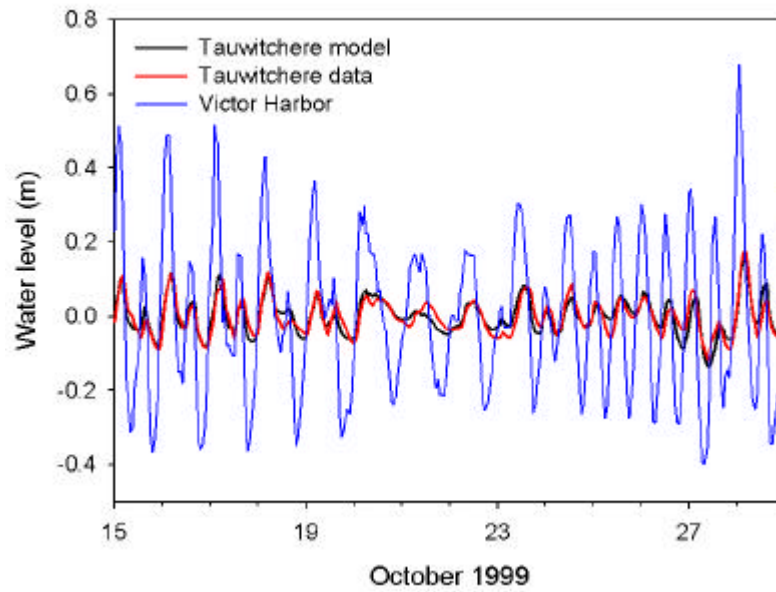


**Figure 12. High-pass filtered modelled and measured water levels at Tauwitchere. Also shown are filtered measured water levels for Victor Harbor.**

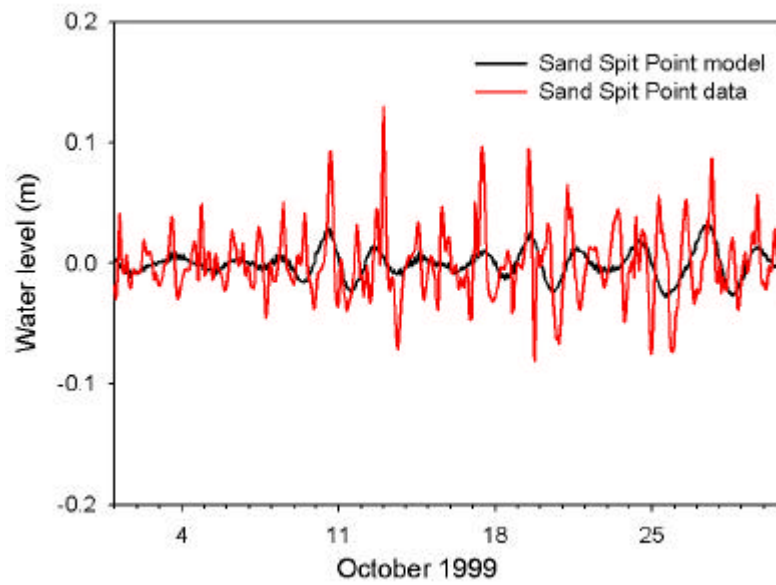


**Figure 13. High-pass filtered modelled and measured water levels at Sand Spit Point.**

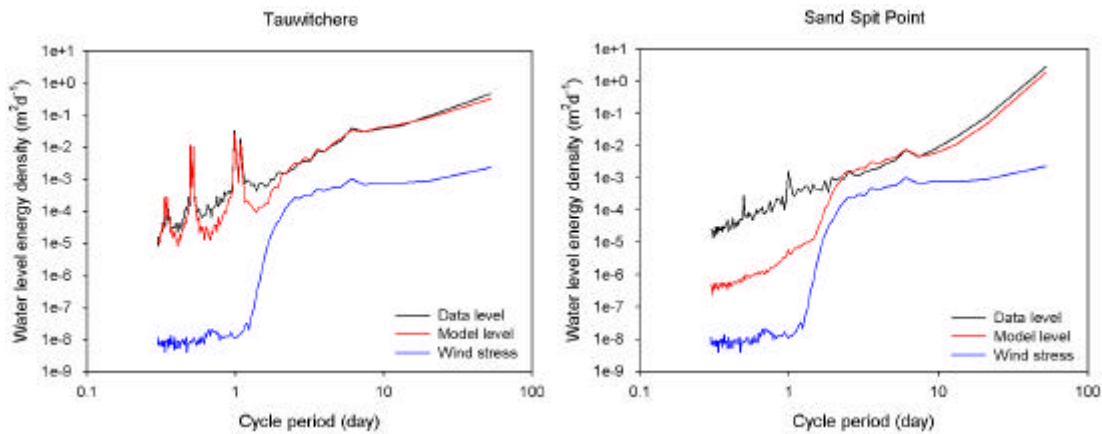


**Figure 14. Spectra of measured and modelled water levels at Sand Spit Point and at Tauwitschere. Also shown are the spectra of the wind stress used to force the model. The units of wind stress energy density are  $\text{N}^2\text{m}^{-4}\text{-day}$ .**

### 3.2. Salinity

Time series of conductivity and temperature were measured by in situ recorders at several sites along the Coorong during the simulation period. From these records, time series of salinity were calculated. Figure 15,

Figure 16 and Figure 17 compare time series of measured and modelled salinity at three locations along the Coorong in order of increasing distance from the Mouth. The discrete measurements also shown are mostly not at the sites of the time series exactly so these salinity data have been interpolated to these sites. The Mark Point, Parnka Point and Sand Spit measurement sites are 19, 62 and 97 km from the Mouth, respectively.

Comparisons between the discrete salinity measurements and the time series show these to be consistent with one another especially when one considers the likelihood of temporal aliasing at times. One such period is the second half of 2001 when rapid oscillations in the measured time series of salinity at Mark Point and Parnka Point would cause doubt of the meaning of a discrete salinity measurement.

Mostly, the model simulations reflect the rapid variation of salinity observed in time series when it occurs. Also, if considering the likely effects of aliasing, the trends in changes in the modelled salinity generally follow the discrete measurements fairly well. At Mark Point, the variation in salinity through the simulation period does not exhibit a smoothly varying seasonal cycle. A seasonal cycle is evident, but salinity changes respond to somewhat irregular barrage outflows. In contrast, at the other end of the system at Sand Spit Point, salinity undergoes a regular seasonal cycle with the highest salinity occurring at the end of summer when salt concentrations are highest due to evaporation (Webster 2005). The model simulations capture this regular variation at least through to 2003.

The salinity record at Sand Spit Point through 2003 to the end of the simulation period is not well represented by the model. The model suggests that peak salinity in 2003 is about 30 higher than in the previous years. The discrete salinity measurements also show a higher salinity; one measurement reached 219, but salinity of less than 100 followed several months later before climbing again to over 150. The sudden drop in salinity in June/July 2003 is not easily explained. The precipitation data for this time did not suggest the occurrence of any significant rainfall events that might lower salinity. The USED inflows occurred after this time so they could not be considered to provide an explanation. The modelled salinity at Sand Spit Point shows smooth variation during this period consistent with previous years, but the discrete salinity measurements at the southern end of the Coorong show erratic variation. This could mean that there are pools of highly saline water formed in the shallow basins to the southeast of Sand Spit Point that pass back and forth past the measurement site. The occurrence of periods of

unusually high salinity in the summers of 2003 and 2004 is captured by the model at the other three sites.

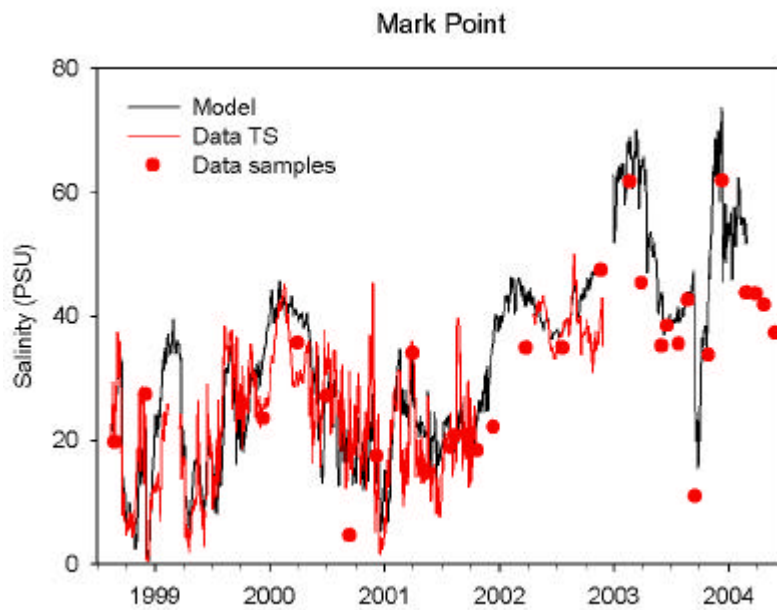


Figure 15. Comparison of measured and modelled salinity at Mark Point.

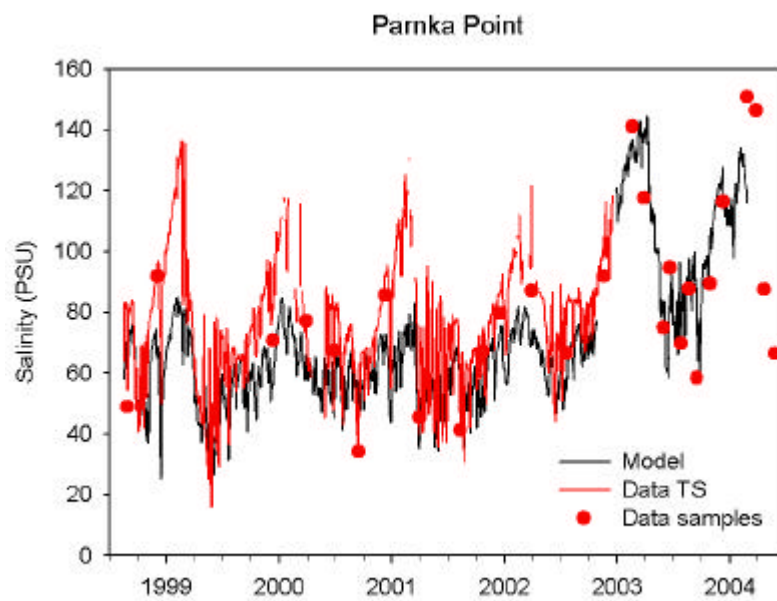
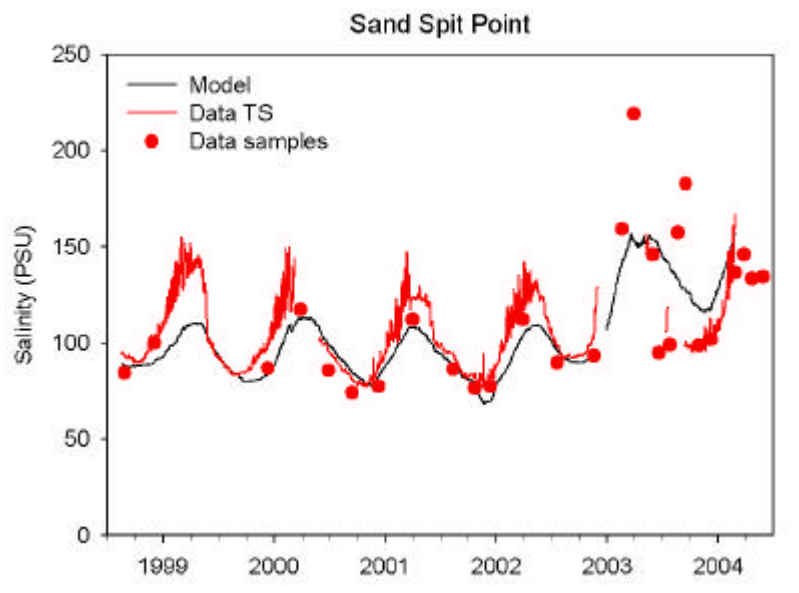
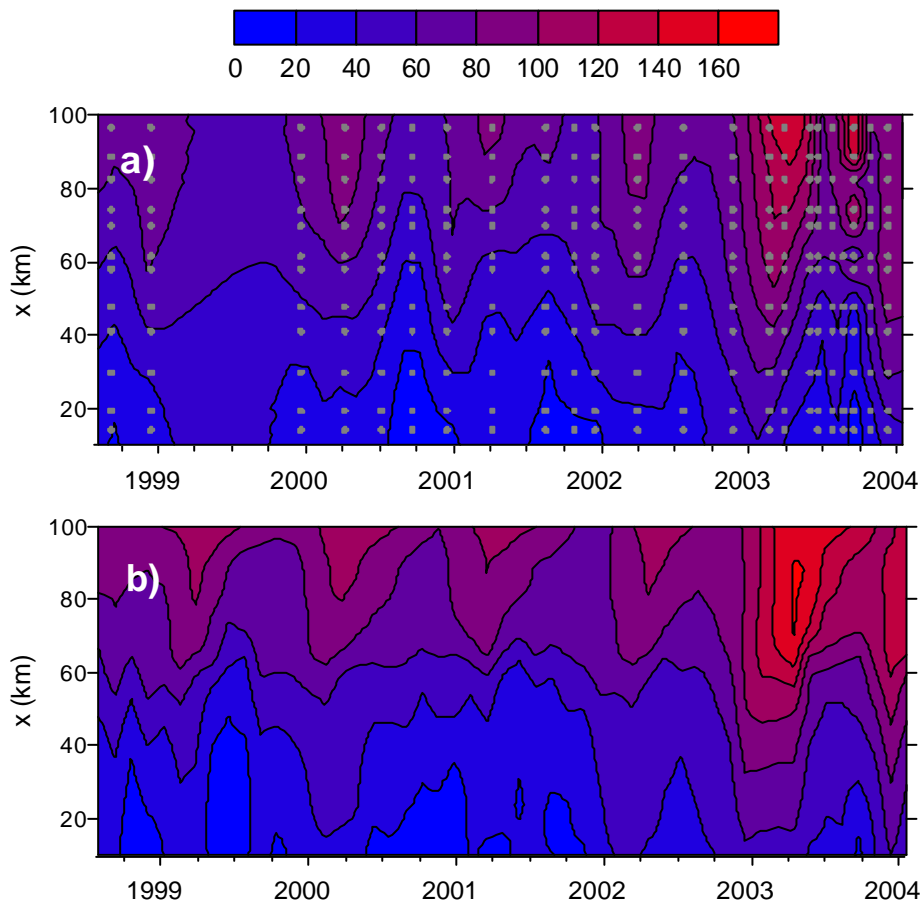


Figure 16. Comparison of measured and modelled salinity at Parnka Point.



**Figure 17. Comparison of measured and modelled salinity at Sand Spit Point.**

The overall pattern of the salinity contours is similar for the model and measurements. Seasonal variation in salinity is significantly greater in the South Lagoon ( $x > 55\text{km}$ ) than in the North Lagoon (Figure 18). The zone of unusually high salinities seen in the time series (Figure 15, Figure 16 and Figure 17) in late summer 2003 penetrates the length of the Coorong. This is a time when there was no inflow from the barrages and the Mouth channel was shallow.



**Figure 18. Contours of salinity through the study period: a) measured salinity b) modelled salinity. In a), the grey dots represent the times and positions of the salinity measurements.**

## 4. Coorong Dynamics

The hydrodynamics of the Coorong has been summarised by Webster (2005) and these dynamics are broadly consistent with what is demonstrated by the model simulations obtained with the hydrodynamic and salinity models described here. In the following discussion, we summarise some of the major features of water flows, water levels and salinity regime as described previously as well as some new inferences obtained from the application of the hydrodynamic and salinity models.

### 4.1. Mouth opening dynamics

Figure 19 shows the estimated Mouth heights and the flow volume through the Mouth over the simulation period. Negative flow indicates outflow and this is mostly due to the barrage discharges with some small contribution from outflows occurring as a consequence of falling sea levels. Positive flows occur during times of rising sea levels and high evaporation during summer. The two periods of strongest outflow in late 1998 and late 2000 coincide with a significant deepening of the Mouth channel. Periods of inflow coincide with the Mouth channel becoming shallower. During 2002 and 2003, the barrage discharges were zero or small and  $Z_M$  increased to  $\sim -0.5$  m. Dredging in the Mouth region to open connections between the Coorong and Goolwa Channels to the sea commenced in October 2002. Fully open channels were achieved in May 2004 and October 2004 for the Goolwa and Coorong Channels respectively. The specifications for the Coorong Channel were for dredging to an average depth of 3 m and width of 80 m. It is likely that the effective channel depths as suggested in Figure 19 were impacted by dredging from October 2002 onwards and that the steady increase seen in the estimated depth of the Mouth channel in late 2003 and early 2004 is a consequence of the channel being opened by dredging.

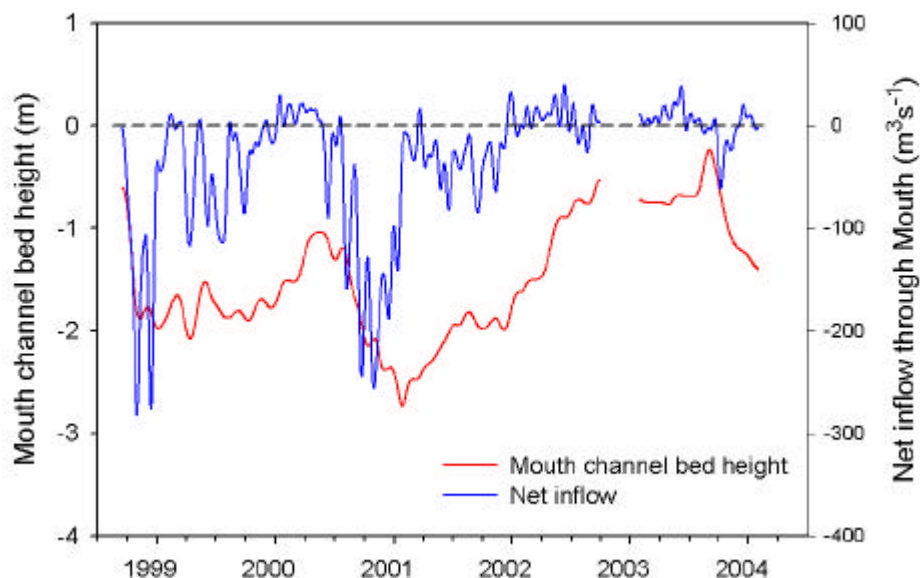


**Figure 19. Time series of estimated heights of the Mouth channel bed ( $Z_M$ ) and modelled flows through the Mouth. Both records have been low-pass filtered with a cut-off period of 28 days.**

We propose a simple model for describing the relationship between the bed height of the Mouth channel ( $Z'_M$ ) and flow speed ( $u_M$ ) through the Mouth as:

$$\frac{dZ'_M}{dt} = \alpha |u_M|^\beta + \gamma. \quad (10)$$

The first term on the left is the rate of change of bed height with time,  $u_M$  is flow speed, and  $\alpha$ ,  $\beta$ , and  $\gamma$  are constants determined by least squares fitting the time series obtained from the time integration of Equation 10 to the time series of  $Z'_M$  estimated using the procedure outlined previously. In this equation, we set  $\alpha$  to be negative if  $u_M$  is negative and  $\alpha$  to be positive if  $u_M$  is positive. The values of the parameters are  $\alpha = \pm 0.019 \text{md}^{-1}$ ,  $\beta = 1.7$ , and  $\gamma = 0.003 \text{md}^{-1}$  when the units of  $u_M$  are  $\text{ms}^{-1}$ . The sign of  $\alpha$  is that of  $u_M$ .

Figure 20 compares the time series of  $Z'_M$  with  $Z_M$ . We show the results up to the end of 2002 only since dredging is likely to affect channel heights in the record after this time.  $Z'_M$  with  $Z_M$  follow one another overall, but there are many features of detail that are not replicated in the model. There are certainly errors in the estimation of  $Z'_M$ . Also, it is likely that the true infill rate in the absence of appreciable Mouth flows is likely to depend on wave and current conditions in Encounter Bay, a factor ignored in the model. The model has been calibrated against a data record of approximately four years duration. How well Equation 10 applies to other times and can be used as a predictor of Mouth channel bed height is not known and remains to be determined.

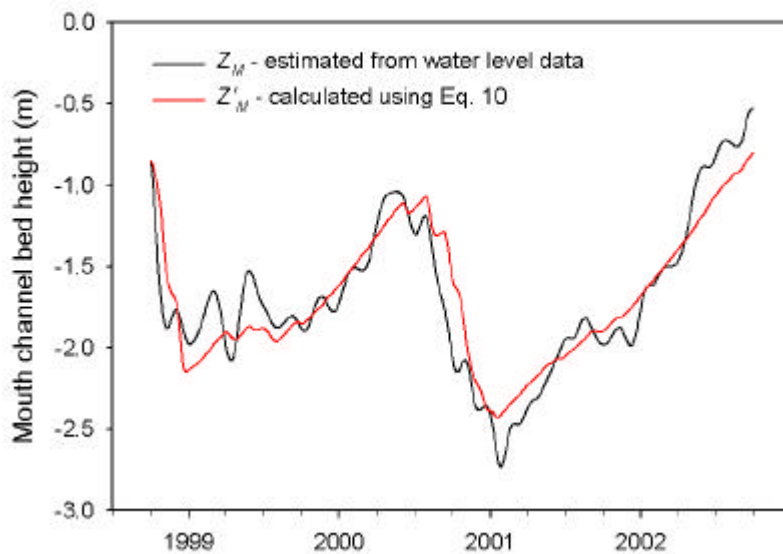


**Figure 20. Comparison of Mouth channel bed heights ( $Z'_M$ ) calculated using Equation 10 with those estimated from the transmission of water level variations to Tauwitschere.**

## 4.2. Water levels

Changes in the water levels in the Coorong can be

'classified into three main types; wind-induced short period changes of a foot or so [sic], with a time scale of days, in which opposite ends of each lagoon move out of phase with each other; short period increases in levels in North Lagoon which occur when the barrages at the north end of the Coorong are opened for several days at a time; and seasonal variations of up to four feet [sic]'.  
Noye 1975

Water level changes in Encounter Bay including tides are also acknowledged as penetrating through the Mouth to influence levels within the Coorong. As has been known previously and confirmed here, water levels in Encounter Bay are not only major drivers of water level variation within the Coorong, but are also major agents of water exchange throughout the system.

### 4.2.1. Tidal water level variation

The tides along the coast of Encounter Bay are described as being micro-tidal in range and semi-diurnal with a moderate diurnal inequality (Short and Hesp 1980). Tidal ranges vary between approximately 1 m during spring tides to approximately 0.2 m during neap tides. When the Mouth is open the tides penetrate through it and cause water level variations in the northern end of the North Lagoon. The degree of attenuation of the energy in the semi-diurnal tide has been assumed to reflect the extent of Mouth opening (Walker and Jessup 1992, Walker 2002). This measure has since been referred to as the mouth opening index or MOI (Close 2002). A more recent analysis by Shuttleworth et al. (2005) uses dynamic equations of the Mouth channel with analytical solutions to infer the area of the Mouth opening as a function of the attenuation of the tidal energy between Encounter Bay and Goolwa Barrage.

Using the model, we can develop the relationship between the height of the Mouth channel ( $Z_M$ ) and the attenuation of tidal energy within the main body of the Coorong. We use a synthetic time series of tidal water levels for Victor Harbor and simulate the resulting response in Coorong levels. The mean water level in the synthetic time series is 0.2 m compared to the 0.21 m average determined from the measured water levels at Victor Harbor. For the simulation, all barrage flows, evaporation, precipitation, wind stress and USED inflows were switched off.

Figure 21 shows the attenuation of tidal energy at Tauwitchere as a function of  $Z_M$  obtained from the model. We refer to this as  $MOI_T$ . The attenuations of the diurnal and semi-diurnal tides are similar to one another. The maximum energy transmission for both tidal frequencies, which occurs for the deepest Mouth channel, is only 0.11–0.12. The amplitude attenuation is the square root of  $MOI_T$  so that even for the deepest Mouth channel the amplitude of the tide at Tauwitchere is reduced by a factor of about three compared to that in the sea nearby. Walker (2002) calculated the tidal energy attenuation for Tauwitchere on a fragmented record of measurements between 1981 and 2000. These  $MOI_T$  showed a significant seasonal attenuation that is associated with the clearing of the Mouth channel by barrage flows. Seasonal maxima mostly reached 0.2 or more. Our maximum  $MOI_T$  is only about half of this value and it occurs for the minimum bed height tested of  $Z_M \sim -3$  m. This suggests that the Mouth channel has filled in over the last decade compared to what it was previously.

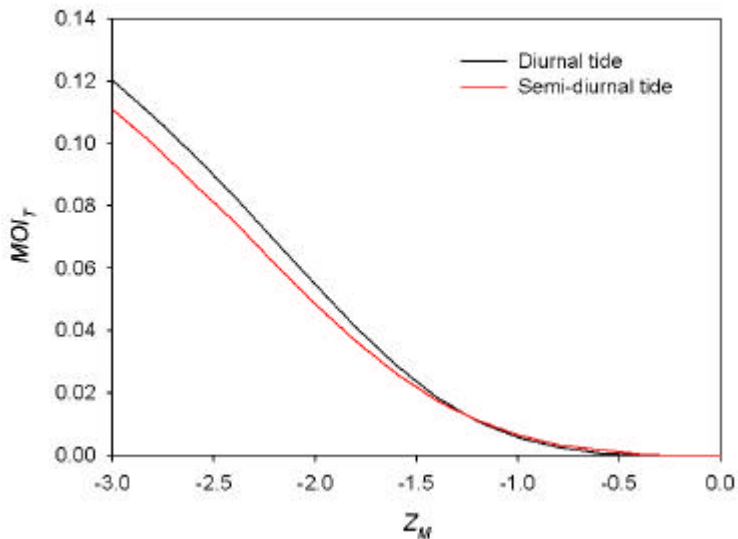


**Figure 21. Attenuation of diurnal and semi-diurnal tidal energy between Encounter Bay and Tauwichee ( $MOI_T$ ).**

Figure 22 shows the penetration of the simulated water level variations for the diurnal and semi-diurnal tides into the North Lagoon. These results were obtained for a deep Mouth channel with  $Z_M = -3.0\text{m}$ . In this plot, the tidal amplitudes at  $x = -1\text{km}$  are the root-mean-square tidal amplitudes for the two tidal constituents in Encounter Bay (Victor Harbor). The tidal amplitudes reduce by approximately 25% through the Mouth channel, but continue to rapidly decrease for the next 14 km or so and then remain fairly uniform at greater distance from the Mouth. Tidal penetration is a function of the interaction between changes in depth and width and loss of energy through bottom friction. These simulations suggest that even with a relatively open Mouth channel, tidal variations over most of the North Lagoon have amplitudes of a few centimetres at most. On this plot, Tauwichee is located at  $x = 10\text{km}$ .

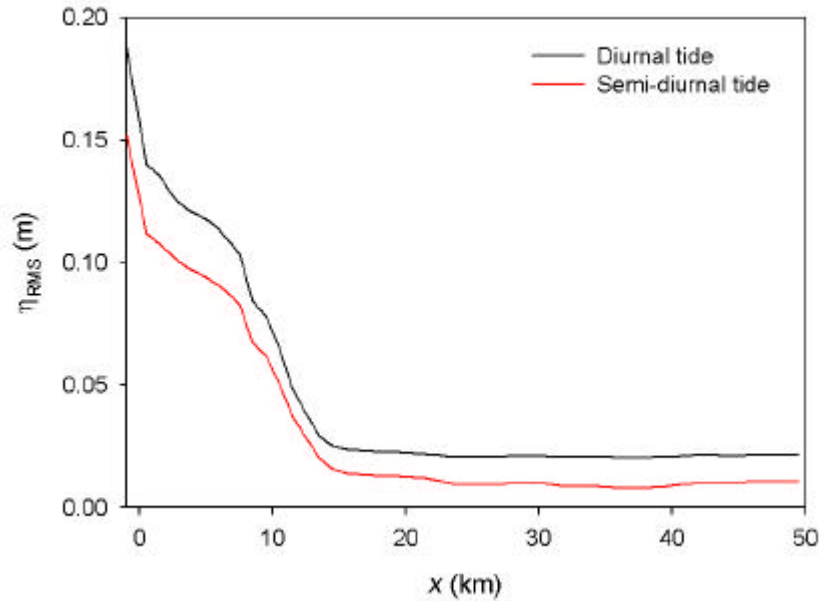


Figure 22. Root-mean-square water level variations for the diurnal and semi-diurnal tides versus distance along North Lagoon. Simulation has  $Z_M = -3.0\text{m}$ .

#### 4.2.2. Wind-driven water level variation

Wind blowing on the water surface of the Coorong exerts a force that pushes water in the downwind direction. This causes the water to pile up against the downwind shore and results in an upwards tilt of the water surface from the upwind to the downwind end. (Figure 23). Once the wind has been blowing for long enough, an equilibrium is established in which the force of the wind on the water surface is counterbalanced by the pressure gradient associated with the water tilting in the opposite direction. If the wind speed drops to zero, then the system relaxes and the currents would flow along the Coorong in the opposite direction.

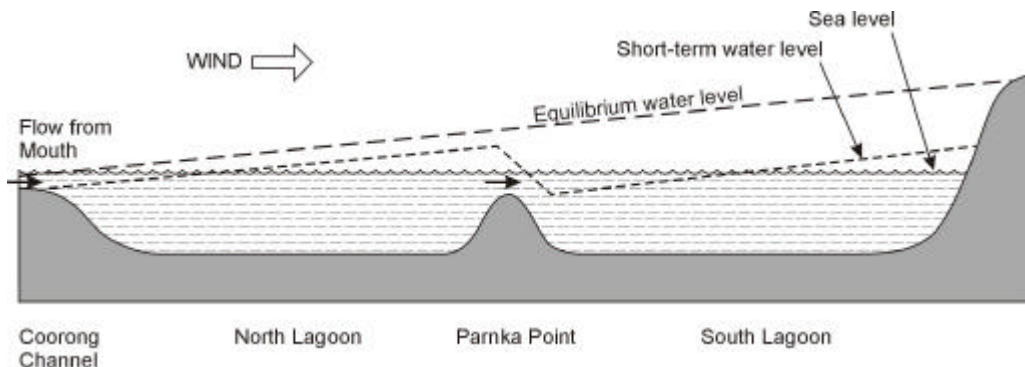


Figure 23. Water level response in the Coorong to and along-channel wind stress.

In the short term (less than a few days), water levels in the North and South Lagoons respond individually, but eventually the entire length of the Coorong tilts in one direction due to flow between the lagoons and filling of the Coorong through the Mouth. At equilibrium, the water level near the Mouth would be that of the sea. Due to the constriction in the Mouth and Parnka Point channels, the initial response of the North and South Lagoons occurs as if these two basins had closed ends. In their analysis of the response of the North Lagoon to wind, Noye and Walsh (1976) treated this lagoon as a closed system and obtained good agreement between their model and measured water levels.

We examine the influence of the wind on water level variation in the system. Figure 24 compares the spectrum of modelled water levels at Tauwitchere with the spectrum obtained when the wind stress is set to zero. At high frequencies, having periods less than about 2.5

days, the spectra converge since the energy in the estimated wind stress is zero at these frequencies anyway. For periods greater than about 10 days, the spectra also converge suggesting that variation at these periods is mainly due to variations in sea level propagating through the Mouth. Between periods of 2.5 and 10 days, the spectra differ demonstrating that wind stress makes a significant contribution to water level variation in this frequency band. Of the water level variance in this period band, 49% appears to be due to the wind which represents an RMS water level fluctuation of approximately 0.05 m in amplitude. For Sand Spit Point, the wind stress contributes 93% of the variance in the 2.5 to 10-day period band. For this location and for this frequency band, the RMS level fluctuation is estimated to be approximately 0.03 m. For periods less than 2.5 days, the model represents wind stress inadequately, but if it is assumed that all the high-frequency variance is due to the wind (see Figure 14), then high-frequency wind variations would be responsible for an additional RMS level fluctuation of approximately 0.02 m at this location.

The schematic representation of the water level fluctuations shown in Figure 23 would suggest that, for longer time period wind stress fluctuations, the response near the southern end of the Coorong (i.e. near Sand Spit Point) would be greater than that nearer the Mouth (i.e. near Tauwitschere). For periods greater than approximately 10 days, the component of the spectrum due to wind forcing diminishes for Tauwitschere but is maintained for Sand Spit Point.

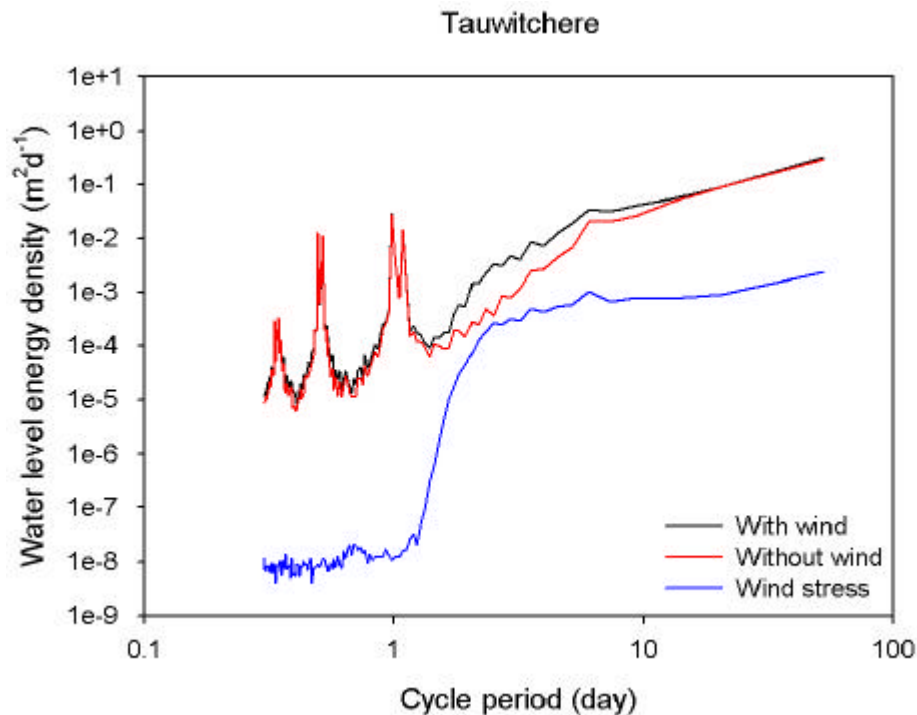


**Figure 24. Spectra of modelled Tauwitschere water levels with and without wind stress. Also shown is the spectrum of the wind stress used to force the model. The units of wind stress energy density are  $N^2m^{-4}$ -day.**

### 4.2.3. Low-frequency water level variation

Low-frequency water level changes in Encounter Bay are characteristically of two types according to Provis and Radok (1979). The first type is due to the passage of weather systems and associated continental shelf waves. These have periods between 1 and 20 days. The second type of fluctuation having periods between 20 to 365 days have an uncertain origin, but appear to be due to sources in the Southern Ocean or in the interaction between the continent and this ocean.

For a water level fluctuation of given amplitude within an enclosed basin such as the Coorong, a high-frequency fluctuation must exchange the same volume of water more quickly than a low-frequency fluctuation. Since the friction associated with a current is approximately proportional to the flow speed squared, a greater frictional force must be overcome in a connecting channel such as the Mouth channel for a high-frequency level fluctuation to occur than for a low-frequency one. Consequently, low-frequency water level variations in Encounter Bay such as those associated with the passage of weather systems penetrate more effectively through the Mouth and along the Coorong than more rapid level fluctuations such as those due to the tides. This behaviour is illustrated in Figure 25 where the attenuations of the energy in level oscillations of 2.5-day and ten-day periods are presented as functions of the bed height of the Mouth channel,  $Z_M$ . For a fully open Mouth, the energy of the ten-day fluctuation is 69% of that in Encounter Bay, but this decreases to 33% for the 2.5-day oscillation. As one would expect, the penetration of the oscillation diminishes as the Mouth channel shallows and is close to zero when  $Z_M \sim 0$ .

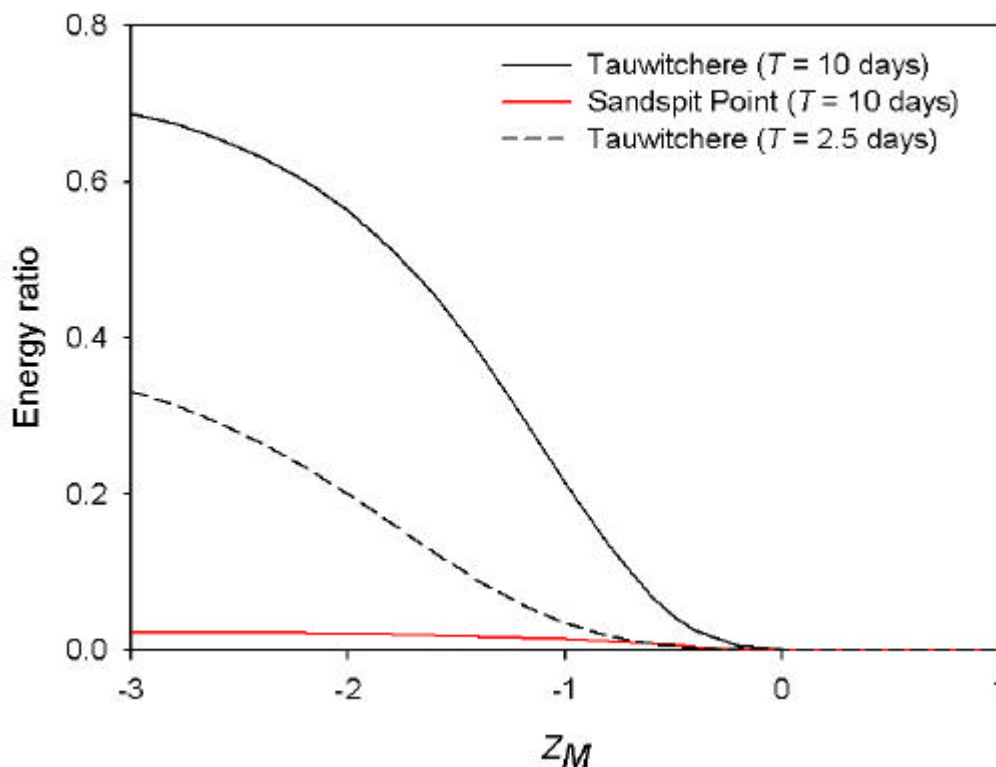


**Figure 25.** Transmission of the energy in water level fluctuations of 0.1 m amplitude (Encounter Bay) with 2.5 and ten-day periods at Tauwitchere and at Sand Spit Point. These results are calculated for a mean sea level of  $\bar{h}_{EB} = 0.2\text{m}$ .

For a Mouth height of  $Z_M = -0.5\text{m}$ , only 4% of the Encounter Bay energy is transmitted to Tauwitchere for the 10-day period versus 0.2% for the diurnal tide (see Figure 21). The reduction in energy transmission is 20 times greater for the higher frequency than for the lower

frequency for this  $Z_M$ , but for  $Z_M = -3.0\text{m}$ , the ratio is 5. Assuming that the amount of energy in water level fluctuations at Tauwitchere due to wind remains independent of Mouth opening depth and that this energy confounds the estimation of  $Z_M$  when this height is large, then one might expect that the calculation of  $Z_M$  using the low-frequency analysis would become relatively more reliable than the high-frequency calculation as the Mouth shallows. This is the argument used to justify the use of the low-frequency analysis instead of the high-frequency analysis for estimating Mouth channel bed height when the channel is shallow (see Section 2.4.1).

Figure 25 also shows the energy transmission for the ten-day oscillation near the southern end of the South Lagoon at Sand Spit Point. The maximum energy penetration occurs for the deepest Mouth channel  $Z_M = -3.0\text{m}$  and the penetration diminishes for decreasing Mouth channel depths. For  $Z_M = -3.0\text{m}$ , the relative energy penetration is 2% which is equivalent to an attenuation in the amplitude of the ten-day fluctuation of 15%. At lower frequencies, the energy transmission becomes more efficient. Figure 26 shows the relative energy transmission to Sand Spit Point for three values of the mean sea level in Encounter Bay for an oscillation period of 90 days. Penetration of level energy into the South Lagoon depends significantly on mean sea level (Figure 26). For  $Z_M < -1\text{m}$ , the penetration is governed primarily by the flow dynamics through Parnka Point channel. For larger values of  $Z_M$ , attenuation through the Mouth is the main factor governing the penetration of level energy to Sand Spit Point. This analysis demonstrates how water levels and motions within the South Lagoon are governed by mean sea level in Encounter Bay. It follows that that seasonal water level changes in Encounter Bay impact on levels and also exchanges at lesser frequencies.

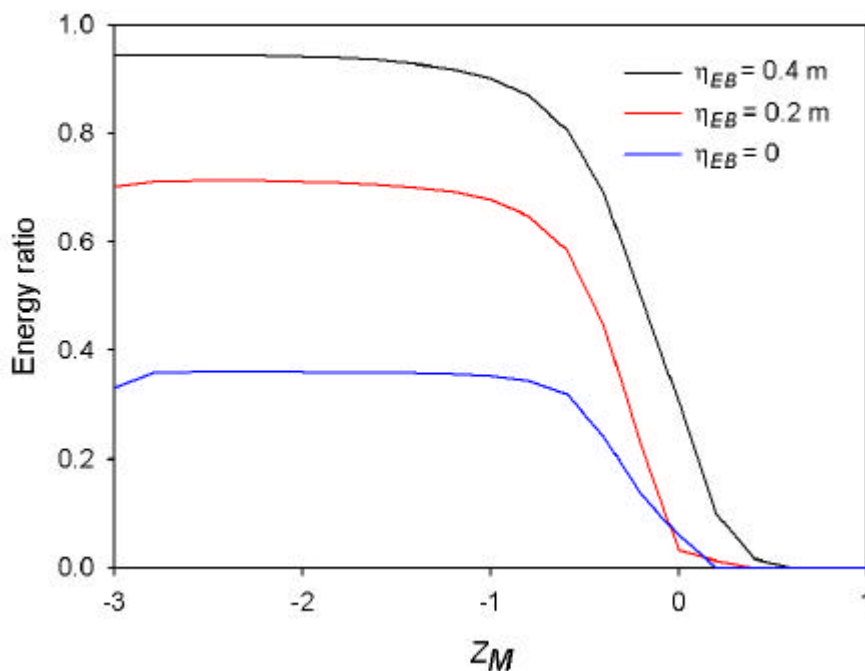
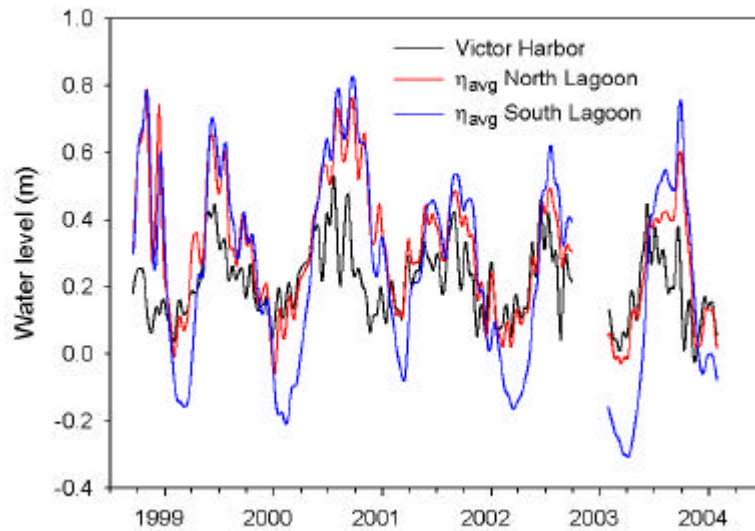


Figure 26. Energy attenuation of water level fluctuations of 0.1 m amplitude (Encounter Bay) to Sand Spit Point for an oscillation period of 90 days. Results are shown for three values of mean sea level in Encounter Bay.

### 4.3. Water budgets in lagoons

Figure 27 compares measured low-pass filtered water levels for Victor Harbor with modelled water levels averaged along the lengths of the North and South Lagoons. Figure 28 and Figure 29 present the inflows represented in the model for the North and South Lagoons. The barrage inflows are combined for the Tauwitchere and Ewe Island Barrages. The flow through the Mouth and Parnka Point channels are model results. Precipitation – evaporation is the rate of water input to the lagoon estimated from pan measurements with the derived pan factor (0.78) applied to the evaporation rate. For clarity of presentation, precipitation – evaporation has been omitted for the North Lagoon flows, but this flow is approximately 75% of that presented for the South Lagoon.



**Figure 27. Measured water levels at Victor Harbor and modelled water levels averaged over the lengths of the North and South Lagoons. The water levels have been low-pass filtered with a cut-off period of 30 days.**

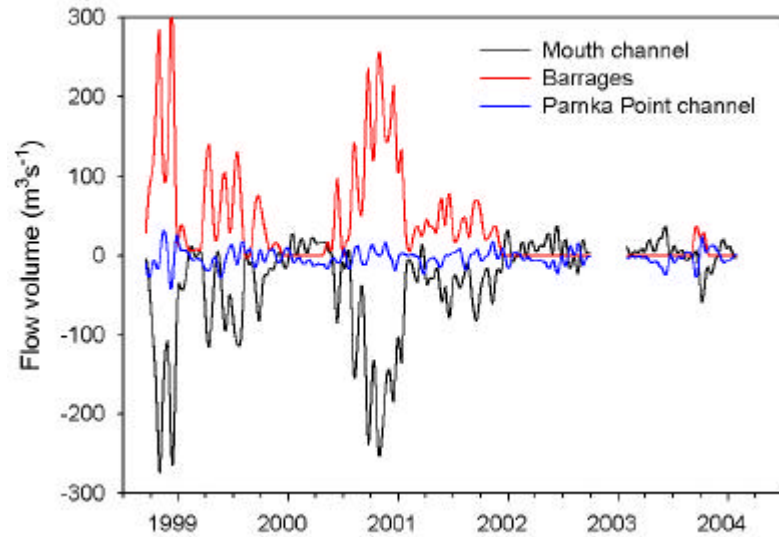


**Figure 28. Flow volumes for inflows to the North Lagoon. Negative values represent flow out of the lagoon. The time series have been low-pass filtered as in Figure 27.**

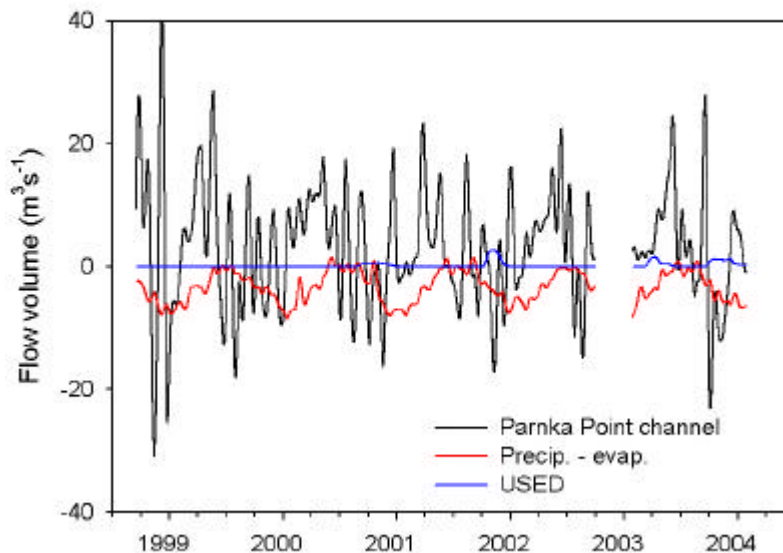


**Figure 29. Flow volumes for inflows to the South Lagoon. Negative values represent flow out of the lagoon. The time series have been low-pass filtered as in Figure 27. Note the difference in scale with Figure 28.**

As has been noted by Webster (2005), the water levels at Victor Harbor undergo a pronounced seasonal cycle that penetrates into both lagoons. The extra hydraulic head associated with elevated barrage outflows causes a further increase in water level during mid to late 1999, 2000 and 2001. In 1999 and 2001, when the largest barrage flows in the record shown were experienced (Figure 28), water level increased in both lagoons to approximately 0.5 m above the water level at Victor Harbor. These are model results, but we have shown that modelled levels at Tauwitche and at Sand Spit Point are a good reflection of measurements where the latter are available (see Figure 10 and Figure 11). Flows through the barrages were virtually zero through 2002 and most of 2003 yet there is a suggestion that water levels in mid to late in the year were higher in the North and South Lagoons than those at Victor Harbor. By switching the wind off in the model, we can ascertain that part of this elevation is explained by the wind tending to tilt the water surface upwards towards the southeast (Figure 23). Also, it would appear that the Mouth channel was quite restricted through this time period (Figure 9). Water levels within the Coorong would have tended to 'hang-up' compared to those in the nearby sea.

During the summer months, water levels in the South Lagoon dropped significantly below those in the North Lagoon due to evaporative water loss. Water levels at Victor Harbor are low by the beginning of summer due to their seasonal cycle and these water levels are transmitted along the length of the Coorong. The constricted channel between the North and South Lagoons becomes shallow and is not able to sustain the flows to the South Lagoon necessary to balance evaporative losses. Pulses of water are delivered through this channel to the South Lagoon by favourable wind tilting in the North Lagoon and by short-term sea level variations, but these are insufficient to prevent the water level from decreasing during the summer. Significant inflows to the South Lagoon appear to coincide with increased water levels in the North Lagoon at the end of summer following the seasonal increase in water level at Victor Harbor.

Figure 28 shows that most of the inflow from the barrages is balanced by an outflow through the Mouth of virtually equal size. The water level increase associated with the barrage inflows also causes a modest flow (compared to the barrage flows) into the South Lagoon through Parnka Point channel. The flows between the lagoons are best represented in Figure 29 where the scale is expanded compared to Figure 28. Close examination of Figure 28 and Figure 29 show that the flow between the lagoons responds to changes in the barrage flows; that is, if the barrage flow is continuously changing, exchange flows will result. Other important causes of flows between the two lagoons are sea level rises and falls, and the wind. At the present time, inflows from the USE drainage area are only small components of the water budget for the Coorong.

#### **4.4. Salinity dynamics**

As represented in the salinity model, the salinity regime in the Coorong is determined by the transport of salt by:

- currents along its length;
- net evaporation; and
- the input of salt through the Mouth and USE drainage.

Along the length of the system, evaporation tends to cause the salt concentration to increase over time. The loss of water through evaporation requires a replacement flow along the Coorong which carries saltwater with it since most commonly the water everywhere is saline except perhaps during times of barrage discharge when water near the northern end might be quite fresh. Conversely, long-Coorong mixing processes transport salt towards the Mouth since mixing processes tend to transport salt from areas of high concentration to areas of lower concentration. Ultimately, the salinity levels and distribution in the system are determined by the balance between 'forward' transport of salt in the flow required to replace evaporation (transport towards the southeast) and the 'backward' mixing of salt by oscillatory currents induced by the wind, barrage flows and sea level changes. This simple conceptual model does not include the contribution by the USE drainage to transport along the Coorong which is small with present drainage flows. In effect, the drainage flow introduces salt into the south-east end of the South Lagoon, but it does induce a long-Coorong flow towards the Mouth which has the net effect of transporting salt out of the system and lowering salinity overall.

Seasonal variations in salinity result from seasonal variations in evaporation rates and long-Coorong transport. Thus, salinity in the South Lagoon tends to increase during summer when evaporation rates are highest and when low sea levels restrict flow past Parnka Point and thereby limit the influx of lower salinity water to replace evaporative losses. Later, sea levels rise and water of lower salinity flows into the South Lagoon and salinity falls.

The mixing or dispersion incorporated in the model has two sources. One is numerical dispersion which arises as a consequence of the implementation of the model on a spatial grid. Dispersion from this source is proportional to the grid cell spacing and the size of the velocity fluctuations (see Appendix C). Although numerical dispersion is strictly a computational artefact as it appears in the model, it has a physical analogy in shear dispersion (Taylor 1953, Young

and Jones 1991). In shear dispersion, diffusion perpendicular to a flow which has lateral variation in velocity results in dispersion along the flow. Lateral transport of a solute to slower or quicker parts of the flow results in solute moving along the channel at different speeds and so results in a spreading of solute in the flow direction. In the context of a channel such as the Coorong, shear flows occur in several ways. Wind blowing on the water surface results in the surface layer moving faster or perhaps in the opposite direction to deeper water layers. Due to shallower depths and to wall friction, flow along the sides of a channel generally has lower speeds than near the centre. Even in a channel of uniform depth, friction slows the flow as the bottom is approached.

For dispersion along a channel in which the flow speed varies laterally, Mackenzie and Roberts (2003) present an analysis for which  $D_s = U^2 W^2 / 120\kappa$  where  $D_s$  is a shear dispersion coefficient,  $U$  is a characteristic flow speed,  $W$  is channel width, and  $\kappa$  is the diffusivity. We take  $\kappa \sim u.H$  where  $u$  is the friction velocity. For flow over the bottom,  $u \sim U/30$  so:

$$D_s \sim \frac{UW^2}{120H}. \quad (11)$$

With  $U \sim 0.03\text{ms}^{-1}$ ,  $W = 1.8\text{km}$  and  $H \sim 1.5\text{m}$  for the Coorong,  $D_s$  is calculated as  $540\text{m}^2\text{s}^{-1}$  compared to  $73\text{m}^2\text{s}^{-1}$  which is the average numerical dispersion coefficient calculated using the method outlined in Appendix C. For matching the measured salinity distribution along the Coorong, we added additional dispersivity with a coefficient value of  $37\text{m}^2\text{s}^{-1}$  so that the effective magnitude of the dispersivity used in the model is  $\sim 110\text{m}^2\text{s}^{-1}$ . We suggest that the discrepancies between the two estimates of the dispersion coefficient are probably due to the simplifying assumptions used to derive  $D_s$ . Mackenzie and Roberts assume a parabolic velocity profile across the channel which is certainly a gross simplification for the Coorong. Also, we have estimated the lateral turbulent diffusivity as  $\kappa \sim u.H$ , a value that is certain to underestimate the true value significantly. However, the significance of this analysis is that  $D_s$  is proportional to  $U$  in Equation 11 as it is in the expression derived for the magnitude of numerical dispersion in Appendix C.

We have assumed that transport along the Coorong has been primarily due to water level changes and to the wind stress acting on the water surface. Another possible mechanism for salt transport along the Coorong is advection established by longitudinal density gradients in the water column. In such a system, relatively fresh water would flow as a surface layer along the Coorong towards the southeast over a more saline layer flowing in the opposite direction. Holloway (1980) identified several occasions during a year-long study undertaken at Long Point when salinities in the surface layer were markedly different from those in the deeper part of the water column. Long Point is located approximately mid-way between the Mouth and Paraka Point. Stratification development is attributed to the advection of a relatively fresh layer on top of an existing brine layer or from the advection of a brine layer beneath an existing fresher layer. Overall, one might expect the brine layer to originate towards the southern end of the North Lagoon and perhaps even from the South Lagoon, whereas the fresher layer could result from either freshwater flows over the barrages or from seawater originating from the Mouth. Based on the results of intermittent surveys, Geddes (1987) noted that the water column was usually isohaline, but there were occasions when significant stratification was measured. More recent measurements at a series of stations along the North Lagoon by Geddes (2005) showed the lagoon to be mostly vertically mixed in salinity during transects in September 2003 and July 2004, but significant vertical stratification was evident along most of the lagoon length in April 2004. The model cannot accommodate such density-induced transport explicitly. Any such transport must be incorporated implicitly in long-Coorong dispersion.

We illustrate features of the salinity dynamics in the Coorong by comparing the model simulations using measured inflows and estimated  $Z_M$  with two scenarios for which the barrage and USED inflows are assumed to be zero. Since early 2002, these flows have been very small and with the current drought conditions in the Murray–Darling Basin, releases from the barrages

are likely to be small for the near future. From Figure 19, it would seem that the period of low flows since 2002 have resulted in a Mouth channel bed height of  $Z_M \sim -0.5\text{m}$  so this might be expected to be the  $Z_M$  attained after a prolonged period of low barrage discharge without dredging. We consider one scenario to have  $Z_M = -0.5\text{m}$  and the other to have  $Z_M = -2.0\text{m}$ . The latter scenario is no flow, but the Mouth channel is assumed to be maintained at this height through dredging. The average modelled salinities in each lagoon for the simulation including barrage flows are compared to those for the two scenarios in Figure 30 and Figure 31.

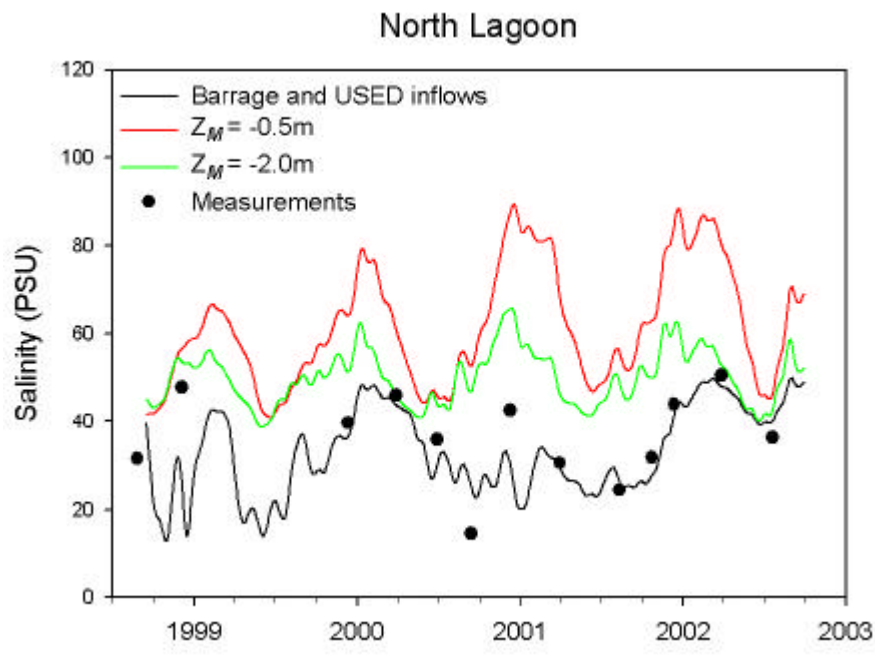


**Figure 30. Average modelled salinity in the North Lagoon for three simulations: 1) barrage and USED inflows and variable  $Z_M$ ; 2) no inflows and  $Z_M = -0.5\text{m}$ ; and 3) no inflows and  $Z_M = -2.0\text{m}$ . Also shown is average measured salinity in the North Lagoon calculated from the periodic sampling transects.**

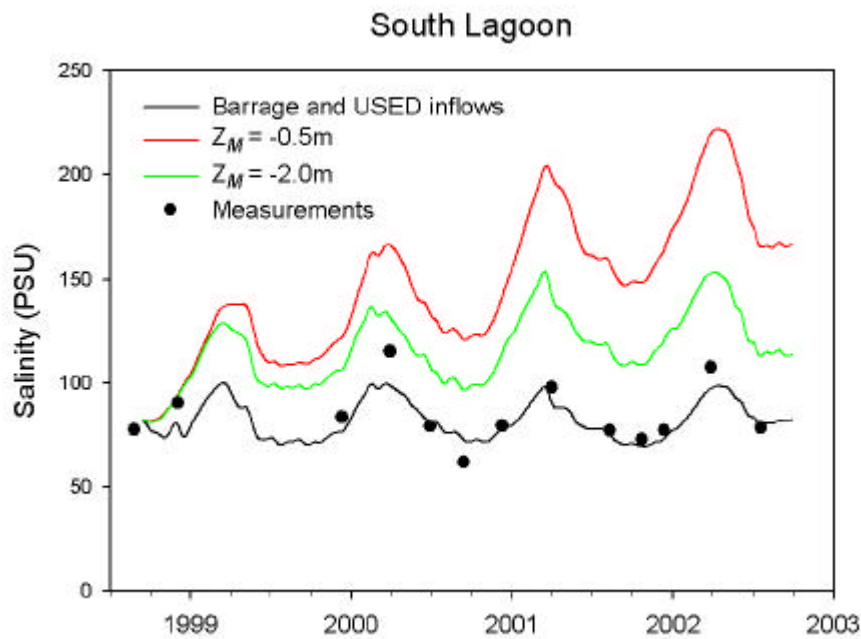


**Figure 31. Average modelled salinity in the South Lagoon for three simulations: 1) barrage and USED inflows and variable  $Z_M$ ; 2) no inflows and  $Z_M = -0.5\text{m}$ ; and 3) no inflows and  $Z_M = -2.0\text{m}$ . Also shown is average measured salinity in the North Lagoon calculated from the periodic sampling transects.**

The barrage flows in late-1998, mid-1999 and mid 2000 have the clear effect of depressing average salinity in the North Lagoon. However, it is apparent that salinity in the North Lagoon also responds to sea level change. This is demonstrated clearly by the drop in salinity in the North Lagoon starting in early 2000. This drop precedes the barrage inflow of that year, but it does coincide with the influx of seawater of lower salinity than ambient Coorong water as the seasonal sea level rises.

The effect of having no flows in the no-flow two scenarios is for a virtually immediate increase in the salinity in both the North and South Lagoons. The start of the simulation period coincides with spring and salinity increases during the following months due to evaporation. In the following years, salinity undergoes a pronounced seasonal cycle in both lagoons due to cycle of high evaporation in summer followed by replenishment by water of lower salinity later in the year as sea level rises. For the no-flow scenarios, salinities in both lagoons are mostly substantially higher than those with flows. The  $Z_M = -2.0\text{m}$  scenario shows similar salinity in the North Lagoon after early 2002 to the non-zero inflow case, but after this time barrage flows to the Coorong were very small anyway. Salinities in the South Lagoon were substantially higher than for the non-zero flow case and were continuing to rise overall for  $Z_M = -0.5\text{m}$  at the end of the period of simulation. For this scenario, it is evident that the oscillatory flows through Parnka Point channel ultimately arising from sea level variations were significantly reduced by the constricted Mouth channel. Exchange along the lengths of the lagoons and between them was reduced allowing salinity levels in the South Lagoon to increase beyond those that are predicted to occur for a deeper Mouth channel.

## 5. Summary and Conclusions

The main purpose of this report has been to describe the hydrodynamic and salinity models and their application to the Coorong in order to form a basis for future model evaluation of scenarios. The report also uses model applications to elucidate features of the physical dynamics of the Coorong. The hydrodynamics model is a conventional one-dimensional model designed to simulate the time-varying water levels and currents along the length of the Coorong. It is linear over most of its domain, but incorporates non-linear hydrodynamics in the channel connecting the body of the Coorong to the sea (the Mouth) and in the constricted channel that separates the North and South Lagoons (the Parnka Point Channel). A salt transport model is embedded with the hydrodynamic model for simulating salinity. The inputs to the model are flows through the barrages, evaporation, precipitation, wind, sea level including the tides and flows from the USE drainage area.

The calibration of the model required the estimation of five tunable parameters namely:

- depths of the Mouth channel and the Parnka Point channel;
- effective width of the Mouth channel;
- dispersion coefficient for salinity; and
- a factor used for estimating Coorong evaporation rate from measured pan evaporation rates.

The Mouth channel depths (expressed as the height of the channel bottom) and widths were estimated on a weekly basis by matching the simulated water level response at Tauwitchere to measurements. Calibration for the depth of the Parnka Point channel and of the evaporation factor was accomplished principally by matching simulations of water levels in the South Lagoon and salinities throughout the Coorong with measurements. Overall, the hydrodynamic and salinity models were well able to represent the time series of measured water levels and salinities throughout the Coorong system lending credibility to conclusions that might be drawn about the dynamics of this lagoon system from the models' application.

The application of the models reinforces previous suppositions about the physical dynamics of the Coorong and unveils some new features of their character:

- The depths of the Mouth channel are clearly related to outflow rates through the Mouth. Inflow and outflows to the Coorong are caused by rises and falls in sea level over a range of timescales and by the balance of precipitation and evaporation, but the largest outflows were due to barrage discharges when they occurred. A simple model for predicting Mouth depth is presented that well represents water level variations as a function of Mouth flow over four years of the hydrodynamic model application, but it remains to be tested for other years.
- Within the body of the North Lagoon, at weather timescales (10 days or less), water level variations are caused in similar measure by the wind which tilts the water level one way or another depending on wind direction, and by sea level variations. Tidal water level variations at the diurnal and semi-diurnal frequencies are likely to dominate within approximately 15 km from the Mouth, but the importance of these depends very much on the degree to which the Mouth channel is open. In the South Lagoon, most water level fluctuations at weather timescales are caused by the wind. The hydrodynamic model well represents wind-driven water level variations for periods longer than some 2.5 days, but the meteorological data used in the simulations does not resolve the wind at smaller periods so the higher frequency water level fluctuations in the model simulations are not present.
- Sea level variations with periods longer than a few days penetrate more effectively than shorter period fluctuations into the Coorong and can be important drivers of water level fluctuations in both lagoons. Penetration increases as the period increases, as the

Mouth channel deepens and for higher sea level. Exchange of water through the Parnka Point channel between the North and South Lagoons limits the extent to which sea level variations affect levels in the South Lagoons. When sea level (and water level in the North Lagoon) drops below approximately 0 m (AHD) in summer, water flow through the Parnka Point channel is not able to replenish evaporative losses in the South Lagoon resulting in a further drop there and increased salinity. Water level in both lagoons rises later in the year with the seasonal rise in sea level in autumn.

- The salinity regime in the Coorong is determined by the transport of salt by currents along its length, by net evaporation and by the input of salt through the Mouth and USE drainage. Along the length of the system, evaporation tends to cause the salt concentration to increase with time. The evaporative loss of water in both lagoons requires a replacement flow along the Coorong which carries saltwater with it. At the same time, long-Coorong mixing processes transport salt towards the Mouth. Ultimately, the salinity levels in the system are determined by the balance between 'forward' transport of salt in the flow required to replace evaporation (transport towards the southeast) and the 'backward' mixing of salt by oscillatory currents induced by the wind, barrage flows and sea level changes. The USE drainage inflows were small during the period simulated and are judged to have a small influence on the salinity dynamics. This may not be the case in the future if drainage inflows were to increase substantially.
- The condition of the Mouth channel impacts on the mixing processes within the Coorong and so has a major influence on the salinity regime. When the Mouth is constricted, fluctuations in sea level penetrate less effectively into the Coorong and the exchange flows associated with these fluctuations are reduced. As a consequence mixing of salt back towards the Mouth is less effective and salinity tends to increase in both lagoons.
- The barrage flows influence the salinity dynamics in the Coorong in at least three important ways. Periods of elevated barrage flows deepen the Mouth channel which in turn allows more active mixing along the length of the Coorong. By freshening the water at the northern end of the North Lagoon (compared to sea water), the water that flows along the Coorong to replace evaporative losses has a lower salinity. Even after evaporation increases the salt concentrations in the two lagoons, a lower salinity is maintained. When the barrages flow, the water level in the whole system tends to increase and water is pushed along the Coorong. Generally, variations in discharge cause the water level in the Coorong to rise and fall causing back and forth water exchange along the system which enhances longitudinal mixing.
- The numerical dispersion in the salinity model acts as a surrogate for long-Coorong mixing by shear dispersion associated with oscillatory water motions caused by sea level changes, barrage inflows and the wind. Another possible mechanism for transporting salt is the circulation resulting from horizontal salinity variations in the system. Such density-driven transport might take on the character of dispersion, but the relationship between mixing and oscillatory flows would be different from that which has been assumed implicitly in the model. The model, as we have applied it, may be able to represent salinity distributions well, since the total amount of dispersion specified for the system is approximately correct. However, if flow conditions within the Coorong were to change significantly and if dispersion is not flow-related the way we have assumed it to be, then salinity prediction would be subject to error. Further comparison of model predictions with data sets from other times representing diverse conditions are needed to resolve whether the representation of dispersion in the salinity model is robust.

## 6. References

- Arcement GJ, Jr and Schneider VR 1984, 'Guide for Selecting Manning's Roughness Coefficients for Natural Channels and Flood Plains', US Department of Transportation, Federal Highways Administration Reports no. FHWA-TS-84-204.
- Bowden KF 1965, 'Horizontal mixing in the sea due to a shearing current', *Journal of Fluid Mechanics*, 21: 83-95.
- Computational Fluid Mechanics International (CFMI) 1992, 'Mathematical Modelling of the Hydrodynamics and Salinity in the Coorong Lagoons', Report CNG-1-12-12/92 prepared for the Engineering and Water Supply Department, South Australia.
- CFMI 1998, 'Long-Term Salinity Trends in the Coorong Lagoons', Report NRC-2-06-98 prepared for the Natural Resources Council, South Australia.
- CFMI 2000, 'Long-Term Salinity Trends in the Coorong Lagoons (Part 2)', Report PIR-1-02/2000 prepared for Primary Industries & Resources, South Australia.
- Close A 2002, 'Options for Reducing the Risk of Closure of the River Murray Mouth', Murray-Darling Basin Commission Technical Report 2002/2.
- Condie S and Webster IT 1997, 'The influence of wind stress, temperature, and humidity gradients on evaporation from reservoirs', *Water Resources Research*, 33(12): 2813–2822.
- Crossley AJ 1999, 'Accurate and Efficient Numerical Solutions for the Saint Venant Equations for Open Channel Flow', PhD thesis, Univ. of Nottingham. Available at: [http://etheses.nottingham.ac.uk/archive/00000109/01/ajc\\_thesis.pdf](http://etheses.nottingham.ac.uk/archive/00000109/01/ajc_thesis.pdf)
- Cunge J, Holly F and Verwey A 1980, *Practical Aspects of Computational River Hydraulics*, Pitman Publishing.
- Elliott AJ 1976, 'The circulation and salinity distribution of the Upper Potomac Estuary', *Chesapeake Science*, 17(3): 141-147.
- Ford PW 2007, Review of the Biogeochemistry of the Coorong and Identification of Future Biogeochemical Research Requirements, Water for a Healthy Country National Research Flagship. CSIRO Report Series.
- Geddes MC 1987, 'Changes in salinity and in the distribution of macrophytes, macrobenthos, and fish in the Coorong lagoons, South Australia, following a period of River Murray flow', *Transactions of the Royal Society of South Australia*, 111(4): 173–181.
- Geddes MC 2005, Ecological Outcomes for the Murray Mouth and Coorong from the Managed Barrage Release of September–October 2003, Report Prepared for the Department of Water, Land, and Biodiversity Conservation. South Australian Research and Development Institute (Aquatic Sciences), Adelaide. SARDI Aquatic Sciences Publication No. RD03/0199-2.
- Harvey N 1996, 'The significance of coastal processes for management of the River Murray Estuary', *Australian Geographical Studies*, 34(1): 45–57.
- Holloway PE 1980, *Vertical Temperature Structure in Shallow Water*, PhD thesis, Flinders Institute for Atmospheric and Marine Sciences, The Flinders University of South Australia.
- Lamontagne S, McEwan K, Webster I, Ford P, Leaney F and Walker G 2004, Coorong, Lower Lakes, and Murray Mouth. Knowledge Gaps and Knowledge Needs for Delivering Better Ecological Outcomes, Water for a Healthy Country National Research Flagship CSIRO: Canberra.
- Linacre E 2005, 'Lake Eo, pan Ep, actual (terrestrial) Ea, potential Et and ocean evaporation rates', in RM Gifford. (ed.), *Proceedings of a Workshop Held at the Shine Dome*,

*Australian Academy of Science, Canberra 22–23 November 2004.* p32–40.  
<http://www.science.org.au/natcoms/pan-evap.pdf>

- Mackenzie T and Roberts AJ 2003, 'Holistic discretisation of shear dispersion in a two-dimensional channel', *ANZIAM J.* 44(E): C512–C530.
- Massey BS 1979, *Mechanics of Fluids*, Van Nostrand Rheinhold Company.
- Nielsen P 1988, 'Wave setup: A field study', *Journal of Geophysical Research*, 93(C12): 15,643–15,652.
- NODC (Levitus) 1998, World Ocean Atlas 98. Available at:  
<http://www.cdc.noaa.gov/cdc/data.nodc.woa98.html>.
- Noye BJ 1975, *The Coorong*, Dept. of Adult Education, University of Adelaide, Pub. No. 39.
- Noye BJ and Walsh PJ 1976, 'Wind-induced water level oscillations in a shallow lagoon', *Australian Journal of Marine and Freshwater Research*, 27: 417–430.
- Officer CB and Lynch DR 1981. 'Dynamics of mixing in estuaries'. *Estuarine, Coastal and Shelf Science*, 12(5): 525-533.
- Provis DG and Radok R 1979, 'Sea-level oscillations along the Australian coast', *Australian Journal of Marine and Freshwater Research*, 30: 295–361.
- Roache PJ 1982, *Computational Fluid Dynamics*, 5<sup>th</sup> ed. Hermosa.
- Short AD and Hesp P 1980, Coastal Geomorphology and Hydrodynamics of the South East Coast Protection District of South Australia, Report prepared for South Australian Coast Protection Board.
- Shuttleworth B, Woitd A, Paparella T, Herbig S and Walker D 2005, 'The dynamic behaviour of a river-dominated tidal inlet, River Murray, Australia', *Estuarine, Coastal and Shelf Science*, 64: 645–657.
- Stanhill G 1976, *The CIMO International Evaporimeter Comparisons*, Publication 449 (World Meteorological Organisation, Geneva) 38pp.
- SA Dept. for Water, Land & Biodiversity Conservation 2004, Surface Water Archive 2004, SA Dept. for Water, Land & Biodiversity Conservation. Available at:  
[http://www.dwlbc.sa.gov.au/water/technical/surface\\_water\\_archive/a1pgs/](http://www.dwlbc.sa.gov.au/water/technical/surface_water_archive/a1pgs/).
- Taylor GI 1953, 'Dispersion of soluble matter in solvent flowing slowly through a tube', *Proceedings of the Royal Society Series A*, 219: 186–203.
- Walker DJ and Jessup A 1992, 'Analysis of the dynamic aspects of the River Murray Mouth, South Australia', *Journal of Coastal Research*, 8(1): 71–76.
- Walker DJ 2002, *The Behaviour and Future of the Murray Mouth*, Centre for Applied Modelling in Water Engineering, The University of Adelaide.
- WBM Oceanics 2003, Murray River Mouth – Morphological Model Development Stage 2 – Model Set Up, Calibration and Verification, Report prepared for Murray-Darling Basin Commission & SA Dept. for Water, Land & Biodiversity Conservation. Brisbane, Australia.
- Webster IT, Hancock GJ and Murray AS 1994, 'Use of radium isotopes to examine pore-water exchange in an estuary', *Limnology and Oceanography*, 39(8): 1917-1927.
- Webster IT 2005, An Overview of the Hydrodynamics of the Coorong and Murray Mouth, Water for a Healthy Country National Research Flagship. CSIRO Report Series.
- Young WR and Jones S 1991, 'Shear dispersion', *Phys. Fluids A*. 3(5): 1087–1101.

## Appendix A: Flow through a restricted channel section

When the difference in water level between the ends of the channel is relatively small, the flow speed through the channel is controlled by the difference in water level between the ends. For fixed upstream level, the flow increases as the downstream level decreases. If the level at the downstream end is small enough, then the flow within the channel can become super-critical and further decreases in downstream level have no effect on the volume of the through flow. The channel reaches its maximum discharge capacity (Massey 1979). This phenomenon arises as a consequence of the non-linear second term in Equation 2.

To develop an equation for describing the flow through the constricted sections, we consider the channel section shown in Figure 32. The heights of the water level above the bottom (depths) at the upstream and downstream ends of the channel are  $H_1$  and  $H_2$ , respectively. The channel has length  $L$ , a flat level bottom, and a uniform width  $W$ . The water depths are thus  $H = \eta - Z$ ,  $\eta$  being the water level and  $Z$  the height of the channel bed referenced to AHD.

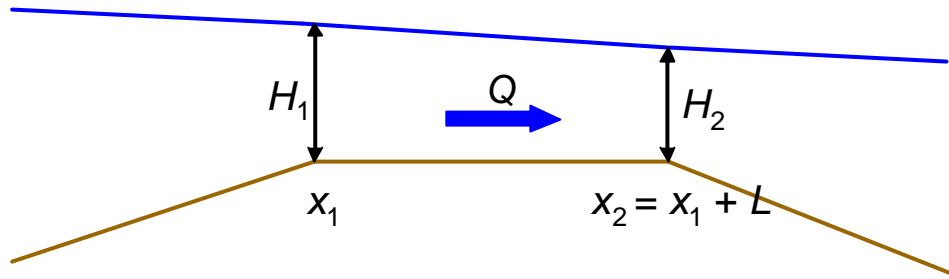


**Figure 32. Constricted channel section.**

We will assume that the channel flow is in quasi-steady-state ( $\partial Q / \partial t, \partial H / \partial t \sim 0$ ) and that the wind stress affect can be neglected. With these assumptions, Equation 2 becomes:

$$\frac{\partial}{\partial x} \left( \frac{Q^2}{A} \right) + gA \frac{\partial H}{\partial x} + \frac{gn^2 Q^2}{AH^{4/3}} = 0, \quad (12)$$

where use is made of Equation 4 and  $Q$  is assumed to be positive. After making the simplifying assumption that  $gn^2 H^{-1/3} \sim gn^2 H_1^{-1/3} = C$  and with  $A = WH$ , Equation 12 can be rearranged and written as:

$$\frac{\partial}{\partial x} \left[ \frac{gW^2 H^4}{4} - Q^2 H \right] + CQ^2 = 0. \quad (13)$$

Integrating this equation between  $x = x_1$  and  $x_1 + L$ , we obtain:

$$\frac{gW^2 (H_1^4 - H_2^4)}{4} - Q^2 (H_1 - H_2) - CLQ^2 = 0 \quad (14)$$

from which:

$$Q = \sqrt{\frac{gW^2 (H_1^4 - H_2^4)}{4(H_1 - H_2 + CL)}} \quad (15)$$

As an example of the application of this equation, Figure 33 shows the calculated flow through the Mouth constriction as a function of water level on its Coorong side. The water level on the ocean side is kept constant at  $\eta_{vH} = 0.5\text{m}$ . Two values of  $Z_M$  are considered. For both values,

the flow through the channel increases as the height difference between the levels in the ocean and Coorong increase until a maximum flow is reached. For a fixed oceanic water level, the maximum flow capacity is higher and occurs at a larger value of the head difference between the channel ends when the height of the channel bed is decreased from  $Z_M = 0$  to  $-0.5$  m.

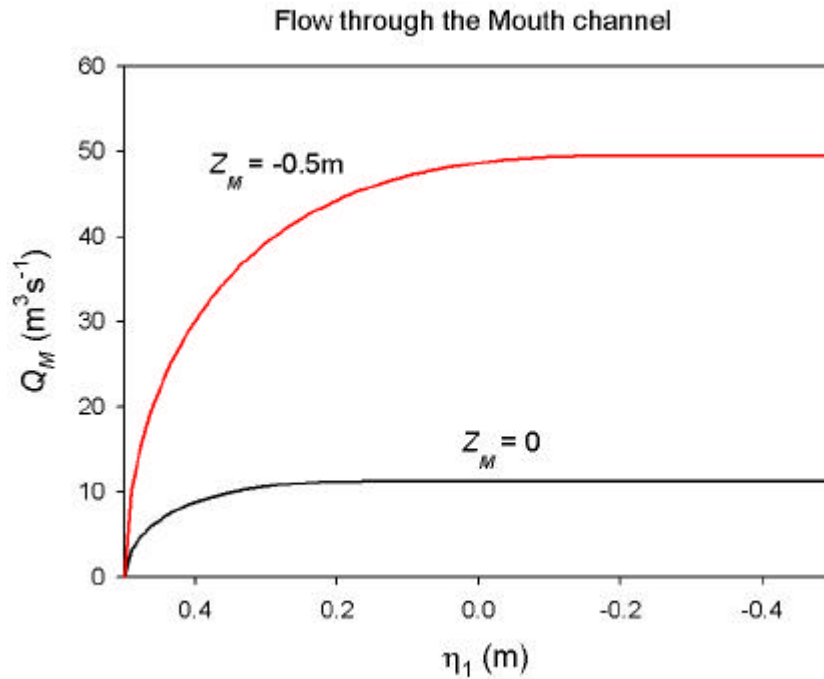


Figure 33. Flows through Mouth channel for two values of the bed height. These flows are calculated using Equation 15. For the results shown, the oceanic water level  $h_{vH} = 0.5\text{m}$  and channel width  $W_M = 100\text{m}$ .

## Appendix B: Data sources

The forcing data used to drive the model were obtained from the sources listed in Table 2. The model required input data at hourly intervals so needed to be manipulated before use.

Data	Location	Organisation	Samp. interval
Water level	Victor Harbor	Flinders Ports, National Tidal Centre, Bureau of Meteorology	hourly
Water level	Coorong	South Australian Dept. of Water, Land & Biodiversity Conservation	hourly
Wind spd./dir.	Meningie	Bureau of Meteorology	2 per day
Evap./precip.	Mundoo	Bureau of Meteorology	daily
Barrage flows	N. Lagoon	Murray-Darling Basin Commission	monthly
USED flows/salinity	S. Lagoon	South Australian Dept. of Water, Land & Biodiversity Conservation	daily
Salinity transects	Coorong	South Australian Environmental Protection Agency / South Australian Dept. of Environment and Heritage / South Australian Dept. of Water, Land & Biodiversity Conservation	1–4 months

**Table 2. Sources of data used in Coorong modelling.**

### *Wind stress*

Wind speed and direction were observed daily at Meningie at 9 am and at 3 pm. These data were interpolated to hourly intervals. The model required a time series of the long-channel component of wind stress to be calculated for Equation 2. Wind stress was estimated using the standard expression:

$$\tau_x = \rho_a C_D U_a^2 \cos(\theta), \quad (16)$$

where  $\rho_a \sim 1.2 \text{ kg m}^{-3}$  is air density,  $C_D \sim 0.0015$  is the aerodynamic drag coefficient,  $U_a$  is wind speed and  $\theta$  is the angle between the wind direction and the alignment of the Coorong channel axis ( $\theta = 130^\circ$  from N).

The comparisons between model-simulated and measured water levels at Sand Spit Point suggested that the wind stress was too low. Matching of the total energy in the spectral response between measured and modelled water levels in the period band 2.5 to 15 days at Sand Spit Point and Tauwichee led to an optimal value for this factor of 2.8. Figure 34 shows a comparison between measured and modelled band-passed water levels with the wind stress factor applied. The figure also demonstrates how wind stress is a major driver of water level fluctuations in this frequency band.

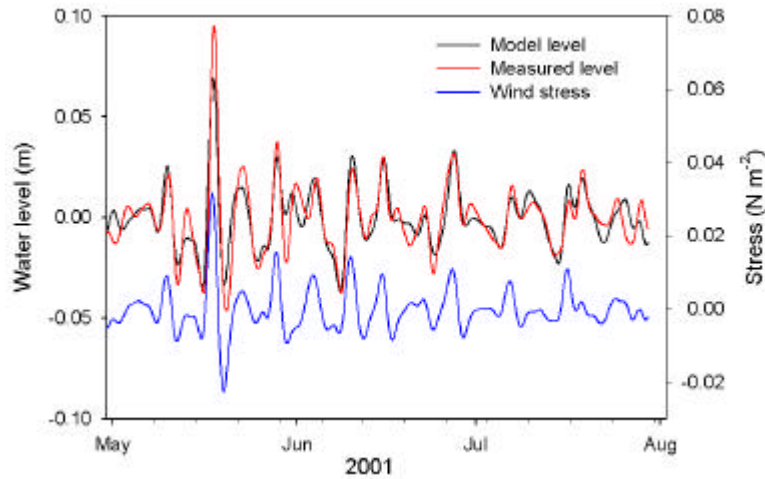


**Figure 34. Band-passed wind stress and band-passed modelled and measured water levels at Sand Spit Point. Low-frequency cut-off period is 15 days and high-frequency cut-off period is 2.5 days.**

The analysis presented in Section 3.1 suggested that wind stress estimated from twice-daily measurements was severely attenuated at periods shorter than approximately 2.5 days. Figure 34 also demonstrates how much if not most of the variance in water level at periods between 2.5 to 10 days is associated with wind stress fluctuations; that is the tilting of the water surface due to the wind. The need to apply a factor of 2.8 to the wind stress suggests that the wind speed is underestimated by a factor of  $\sqrt{2.8} = 1.7$ . Because wind stress is derived from the square of the wind speed, an estimate of stress based on average wind speed will inevitably underestimate the average stress. Also, it might be expected that wind speeds over the Coorong and at Meningie would differ because of their spatial separation.

#### *Barrage flows*

Five barrages separate the Coorong from Lake Alexandrina including Goolwa, Mundoo, Boundary Creek, Ewe Island and Tauwitche. Each barrage has a number of gates and flow through the barrage is enabled by lifting one or more of them. The combined barrage flows have been estimated on a monthly basis from modelling of water balances in the River Murray and Lake Alexandrina since 1963 (Close 2002). The flows through individual barrages have not been measured but daily records have been kept of the number of gates that are open at each one.

Suppose the number of gates that are open on a given day  $d$  for barrage  $i$  is  $G_i(d)$ . The total number of open-gate days summed over all barrages in a particular month is then:

$$G_T = \sum_{i=1}^5 \sum_{d=1}^M G_i, \quad (17)$$

where  $M$  is the number of days in a particular month. With the assumption that the flows through all the gates are the same in a month, then an estimate of the flow through a particular barrage on a particular day ( $Q_i$ ) can be calculated as:

$$Q_i = \frac{G_i Q_T}{G_T}, \quad (18)$$

where  $Q_T$  is the total discharge through all barrages in the month.

## Appendix C: Numerical diffusion

The representation of spatially continuous equations on a spatially discrete grid can lead to diffusion-like transport independently of the presence of explicit dispersion terms in the equations. This phenomenon is numerical diffusion and our solution of the salinity equation for the Coorong is affected by it. Here we examine the consequences of its presence.

We consider two adjoining cells in the salinity grid and the advective transport between them (see Figure 35). Suppose the flow velocity between the cells is sinusoidal with amplitude  $U_0$  and frequency  $\omega$ . With upwind differencing, the flow between the cells is:

$$\begin{aligned}
 u^+ &= U_0 \sin \omega t \text{ for } 0 \leq t < \frac{\pi}{\omega}, \\
 &= 0 \text{ for } \frac{\pi}{\omega} \leq t < \frac{2\pi}{\omega}, \\
 u^- &= 0 \text{ for } 0 \leq t < \frac{\pi}{\omega}, \\
 &= U_0 \sin \omega t \text{ for } \frac{\pi}{\omega} \leq t < \frac{2\pi}{\omega}.
 \end{aligned} \tag{19}$$

The flux of salt to the right is  $F^+ = A S_i u^+$  and the flux of salt to the left is  $F^- = A S_{i+1} u^-$  where  $A$  is the cross-sectional area over the cell interface. We shall assume that the salinities in the two cells  $S_i$  and  $S_{i+1}$  are constant over the cycle in  $u$ . Thus, the exchange between the two cells over one cycle is:

$$\begin{aligned}
 E &= A \int_0^{2\pi/\omega} (S_i u^+ + S_{i+1} u^-) dt, \\
 &= \frac{2AU_0}{\omega} (S_i - S_{i+1}).
 \end{aligned} \tag{20}$$

where use has been made of Equation 19.

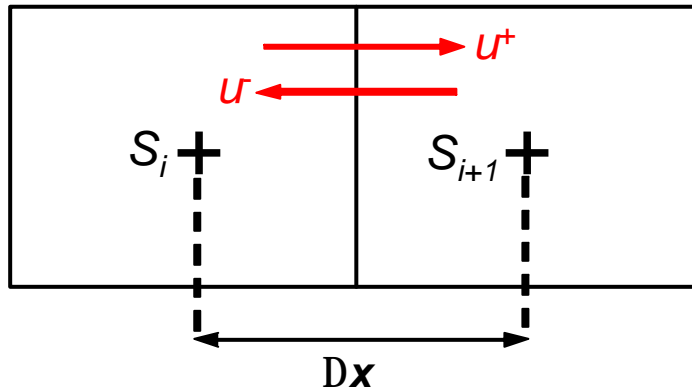


**Figure 35. Advective exchange between two adjacent grid cells in salinity model. The '+' denote the centres of the cells.**

The average flux of salt from left to right over one cycle is  $F = \omega E / 2\pi$  which is

$$\bar{F} = \frac{AU_0}{\pi} (S_i - S_{i+1}). \tag{21}$$

A diffusive flux between cell  $i$  and cell  $i+1$  would have the form:

$$F_D = -AD \frac{\partial S}{\partial x} \quad (22)$$

where  $D$  is the diffusion coefficient. Expressed in numerical form this flux is represented as:

$$F_D = AD \frac{S_i - S_{i+1}}{\Delta x} . \quad (23)$$

Equations 21 and 23 are equivalent if  $D = xU_0 / \pi$ . This  $D$  is the apparent numerical diffusion coefficient that arises from the discretisation of the model domain for equation representation. Roache (1982) derives a similar expression to this for numerical viscosity for the upwind steady-state problem as  $D = xU_0 / 2$ .

For a sinusoidal flow the root-mean-square velocity,  $U_{RMS} = U_0 / \sqrt{2}$ . From the hydrodynamic model solution for the Coorong, we can calculate  $U_{RMS}$  at the cell boundaries of the salinity model and estimate the likely contribution of numerical diffusion to the model solution. The average value of the numerical diffusion coefficient calculated in this way is  $73\text{m}^2\text{s}^{-1}$ . Larger values occur in the channel sections adjacent to the Mouth and Parnka Point. The smallest diffusivities occur at the southern end of the South Lagoon.

